Synaptic plasticity and functional improvement by dopamine transporter internalization after exposure to environmental enrichment

Ji Hea Yu

Department of Medical Science

The Graduate School, Yonsei University

Synaptic plasticity and functional improvement by dopamine transporter internalization after exposure to environmental enrichment

Directed by Professor Sung-Rae Cho

The Doctoral Dissertation
submitted to the Department of Medical Science
the Graduate School of Yonsei University
in partial fulfillment of the requirements for the degree
of Doctor of Philosophy of Medical Science

Ji Hea Yu

June 2016

This certifies that the Doctoral Dissertation's of Ji Hea Yu is approved.

Thesis Supervisor : Sung-Rae Cho

Thesis Committee Member : Chul Hoon Kim

Thesis Committee Member : Jong Eun Lee

Thesis Committee Member : Bae Hwan Lee

Thesis Committee Member : Hyongbum Kim

The Graduate school
Yonsei University

June 2016

ACKNOWLEDGEMENTS

Firstly, I would like to express my sincere gratitude to my advisor Prof. Sung-Rae Cho for the continuous support of my Ph.D study and related research, for his patience, motivation, and immense knowledge. His guidance helped me in all the time of research and writing of this thesis. I could not have imagined having a better advisor and mentor for my Ph.D study.

Besides my advisor, I would like to thank the rest of my thesis committee: Prof. Chul Hoon Kim, Prof. Jong Eun Lee, Prof. Bae Hwan Lee and Prof Hyongbum Kim, for their insightful comments and encouragement, but also for the questions which incented me to widen my research from various perspectives.

My sincere thanks also goes to Ph.D Myung-Sun Kim, M.S Min-Young Lee. Without they precious support it would not be possible to conduct this research.

I thank my fellow labmates : Jung-Hwa Seo, Yoon Kyum Shin, Su Hyun Wi, MinGi Kim and Ah Reum Baek in for the stimulating discussions, for all the fun we have had in the last years.

Also I thank all my friends (too many to list here but you know who you are!) who supported me in writing, and incented me to strive towards my goal.

Last but not the least, I would like to thank my family: my parents and to my younger sisters Ji Young and Ji In for supporting me spiritually throughout writing this thesis and my life in general. Words cannot express how grateful I am to my mother and father for all of the sacrifices that you have made on my behalf. Your prayer for me was what sustained me thus far.

I have dedicated this thesis to mention the above people for their constant support. This accomplishment would not be possible without them. Thank you.

June 2016

Yu Ji Hea

TABLE OF CONTENTS

LIST OF FIGURES

LIST OF TABLE

ABSTRACT

Synaptic plasticity and functional improvement by dopamine transporter internalization after exposure to environmental enrichment

Ji Hea Yu

Department of Medical Science

The Graduate School, Yonsei University

(Directed by Professor Sung-Rae Cho)

Environmental enrichment (EE) with a complex combination of physical, cognitive and social stimulations enhances synaptic plasticity and behavioral function. However, the mechanism remains to be elucidated in detail. Therefore, this study attempted to investigate the underlying mechanisms associated with long-term exposure to EE by evaluating gene expression patterns. After then, this study validated the EE-mediated mechanism of synaptic plasticity. For this, six-week-old CD-1 mice were randomly assigned to either EE or control to investigate functional

outcomes. EE mice were housed in a huge cage (86×76×31 cm^3) for 2 mo, whereas control mice were housed in standard cages (27×22.5×14 cm^3). Motor performances were evaluated using the rotarod test and ladder walking test and gene expression profile was investigated in the cerebral hemispheres using microarray and gene set enrichment analysis (GSEA). Subjects were recruited to evaluate striatal dopamine transporter (DAT) using a [^{18}F]FPCIT-PET, surface DAT using biotinylation assay, DAT phosphorylation using proximity ligation assay (PLA) and immunoprecipitation (IP). In behavioral assessment, EE group showed significantly functional improvement in rotarod performance and ladder walking test. Microarray analysis revealed that genes associated with neuronal activity were significantly altered by EE. GSEA showed that genes involved in synaptic transmission and postsynaptic signal transduction were globally upregulated, whereas those associated with reuptake by presynaptic neurotransmitter transporters were downregulated. In particular, both microarray and GSEA demonstrated that EE exposure increased opioid signaling, acetylcholine release cycle, and postsynaptic neurotransmitter receptors but decreased Na^+/Cl^--dependent neurotransmitter transporters, including DAT Slc6a3 in the brain. Since the striatum receives the largest dopamine input which involved motor performance in the brain, this study investigated that EE-induced functional improvement was related to DAT down-regulation in the striatum. In a [^{18}F]FPCIT positron emission tomography scan, binding values of striatal DAT were significantly decreased approximately 18% in the EE mice relative to the control mice. DAT inhibitor administrated to establish the relationship of the DAT down-regulation to the treatment effects also improved

rotarod performances, suggesting that DAT inhibition recapitulated EE-mediated treatment benefits. Next, EE-induced internalization of DAT was confirmed using a surface biotinylation assay. *In situ* proximity ligation assay and immunoprecipitation demonstrated that EE significantly increased the phosphorylation of striatal DAT as well as the levels of DAT bound with protein kinase C (PKC). In conclusion, EE enhanced motor function through the alteration of synaptic activity–regulating genes, improving the efficient use of neurotransmitters and synaptic plasticity by the downregulation of presynaptic reuptake by neurotransmitter transporters such as DAT. Therefore, this study suggests that EE enables phosphorylation of striatal DAT via a PKC-mediated pathway and causes DAT internalization.

Key words : environmental enrichment, functional improvement, dopamine transporter, internalization, phosphorylation, synaptic plasticity

Synaptic plasticity and functional improvement by dopamine transporter internalization after exposure to environmental enrichment

Ji Hea Yu

Department of Medical Science

The Graduate School, Yonsei University

(Directed by Professor Sung-Rae Cho)

I. INTRODUCTION

Environmental enrichment (EE) is a method of raising animals in a huge cage containing novel objects, such as running wheels and social interaction with a complex combination of physical, cognitive, and social stimulations.[1] The standard definition of EE is 'a combination of complex in animate and social stimulation'.[1] The environment consists of social interactions and stimulation of exploratory and motor behaviour with objects, such as toys, ladders, tunnels and a running wheel for voluntary physical exercise; items which were routinely changed during the experimental period.[2,3]

EE gives rise to biochemical changes and histological improvements such as neurogenesis, axonal sprouting, and dendritic branching, even in the adult brain, consequently promotes behavioral functions.[4,5] EE in normal rodents has several important effects on neurogenesis such as increasing the rate of newborn cell numbers and their survival and affecting the proportion that differentiate into neurons and the proportion that is incorporated into neuronal circuits.[6,7] Concomitant with enhanced neurogenesis, exposure to EE increased levels of synaptic protein such as synaptophysin in the hippocampus of old and young rats.[8]

EE can affect neural plasticity via overexpression of neurotrophic factor and neurotransmitter receptors.[9,10] Studies conducted in rodents have convincingly demonstrated that EE exposure increases the production of neurotrophins such as brain-derived neurotrophic factor (BDNF) and nerve growth factor (NGF) in the cerebral cortex and hippocampus.[9,11] Enhanced expression of neurotrophins and immediate early genes, changes in neurotransmitter receptors, and the activation of cAMP response element–binding protein (CREB) after exposure to EE can affect neural plasticity.[10,12-14] Neural plasticity is a process by which the brain encodes experiences and learns new behaviors and is defined as the modification of existing neural networks by addition or modification of synapses in response to changes in behavior or environment, which can encompass exercise.[1] Neural plasticity includes a wide range of structural and physiological mechanisms including synaptogenesis, neurogenesis, neuronal sprouting, and potentiation of synaptic strength, all of which can lead to the strengthening, repair, or formation of neuronal circuitry.[2]

Importantly, exercise-induced benefits on brain health might help to create the optimum milieu needed for neural plasticity to happen in the injured brain.[7]

Likewise, many reports have shown that EE improves various behavioral performances, suggesting that the positive effects of EE may introduce potential therapeutic strategies for subjects recovering from brain damage.[2,15,16] EE as a rehabilitation therapy could play a role in therapies, either by itself alone or adjuvant to drug treatments or cell transplantation.[3,9,11] According to the previous study, EE enhanced migration and survival of transplanted stem cells toward the injured region after stroke, post-ischemic exercise and EE differentially modulated subventricular zone (SVZ) cell genesis. EE increased the number of endogenous progenitor cells in the SVZ, suggesting that functional recovery can be augmented by environmental factors such as rehabilitation.[9,12] Particularly, enhanced maturation of newly formed cells was seen with EE, raising the possibility that behavioral experience in a complex environment may be used as a rehabilitation strategy following ischemic insult.[9,13] A recent study also showed that EE enhanced endogenous angiogenesis and neurobehavioral functions in chronic hypoxic-ischemia.[17]

As mentioned as the above, EE conditions modify brain plasticity and induce changes on a cellular, molecular and behavioral level.[18,19] The most interesting thing is that an environment affects the dopamine system. Dopamine plays important roles in movement, motor learning, reward, motivation, memory and cognition; therefore dopamine neurotransmitter plasticity could potentially affect these behaviors.[20] It has been established that novel and stressful stimuli within the

environment can induce dopamine release within the prefrontal cortex (PFC) via activation of ventral tegmental area (VTA) neurons.[21-23] The function of VTA dopaminergic neurons that project to the PFC are altered in rodents exposed to EE; namely, stress-induced release of dopamine in the PFC was reduced in rats raised in EE.[24]

Furthermore, dopamine modifies neuronal activity and synaptic transmission in the basal ganglia (BG) in mammals.[25,26] Because the striatum receives the largest dopamine input in the BG in mammals,[25,27] previous studies have concentrated on dopamine effects on striatal neurons. In particular, the dopamine system is involved in motor performance in the BG. [26,28-30]

The previous studies on the relationship between EE and dopamin system have been conducted in the PFC. It has been reported that EE enables a more efficient use of neurotransmitters including dopamine, and modulates DAT dynamics in the PFC.[31,32] However, the underlying mechanism of DAT regulation, including phosphorylation, remains unclear.[33] In particular, the regulation mechanism of DAT after exposure to EE, mainly distributed in the striatum, has not yet to be elucidated.

Therefore, this study aimed to investigate dopamine-related synaptic plasticity underlying functional improvements after EE. This study hypothesized that EE may play a role in the internalization of striatal DAT by the phosphorylation of DAT via a protein kinase C (PKC)-mediated pathway.

II. MATERIALS AND METHODS

1. Environmental Enrichment

The EE mice were housed in a huge cage (86 × 76 × 31 cm^3) containing novel objects, such as tunnels, shelters, toys, and running wheels for voluntary exercise, and allowing for social interaction (10 mice/cage) for 2 mo (Figure 1A), whereas the control mice were housed for the same duration in standard cages (27 × 22.5 × 14 cm^3) (Figure 1B).[34] For all experiments, CD-1 (ICR) mice were housed in a facility accredited by the Association for Assessment and Accreditation of Laboratory Animal Care (AAALAC) and given food and water ad libitum under alternating 12-hr light/dark cycles, according to animal protection regulations. The experimental procedure was approved by the Institutional Animal Care and Use Committee (IACUC) of Yonsei University Health System (permit number: 2013-0209).

2. Experimental grouping

In this study, a total of 20 CD-1 (ICR) mice (Orient bio, Gyeonggi-do, South Korea) were recruited at 6 wks of age. For behavioral assessment, mice were randomly assigned to either EE (n = 10) or standard condition as a control group (n = 10) to investigate functional outcomes. Mice were also recruited to evaluate gene expression by long-term exposure to EE using a microarray (n = 3 per group). Among the subjects, 6 mice were recruited for the PET imaging at 8 wks post-

treatment (n = 3 per group). A total of 6 mice were also recruited to evaluate surface DAT levels using a biotinylation assay (n = 3 per group). For the PLA assay, 8 mice were recruited to evaluate phosphorylation of DAT at 8 wks post-treatment (n = 4 per group). A total of 8 mice were also recruited to confirm phosphorylation of DAT using immunoprecipitation (IP) (n = 10 per group). In order to investigate whether a DAT inhibitor, JHW0007, mediated inhibition could reverse functional outcomes, a total of 20 mice were randomly assigned to either JHW007-treated EE group, JHW007-treated control group, saline-treated EE group or saline-treated control group (n = 5 per group). A schematic timeline of this experiment during the 8 wks is provided in Figure 1C.

Figure 1. Experimental design. (A) CD-1 (ICR) mice were randomly assigned to either environmental enrichment (EE) or the standard condition starting at 6 wks of age for 2 mo. The EE mice were provided a huge cage (86 × 76 × 31 cm^3) containing various objects, such as tunnels, shelters, toys, and running wheels for voluntary exercise, and allowed for enriched social interaction (10 mice/cage). (B) Control mice were housed for the same duration in standard cages (27 × 22.5 × 14 cm^3). (C) A schematic timeline of the experiments.

3. Behavioral assessment

A. Rotarod behavioral test

A rotarod test was used to assess motor coordination and locomotor function. All animals received a pretreatment performance evaluation at 5 to 6 wks of age. For this assessment, mice were placed on a rotarod treadmill (Ugo Basile) (Figure 2A), and the latency of fall, which is the length of time that the animals remained on the rolling rod, was measured. Rotarod tests were then performed at 2-week intervals until 8 wks after the commencement of the treatment at an accelerating speed (4-80 rpm) and a constant speed (64 rpm).[34] The latency period was measured twice for each test, and individual tests were terminated at a maximum latency of 300 s. To avoid any stress related to the tests, we conducted the tests gently.[34]

B. Ladder walking test

The ladder rung walking test allows discrimination between subtle disturbances of motor function by combining qualitative and quantitative analysis of skilled walking.[35] The ladder walking test was performed eight wks after the treatment. In the ladder walking test, the mice were required to walk a distance of 1 m three times on a horizontal ladder with metal rungs (Jeung Do B&P, Gyeonggi-do, South Korea) located at differing distances apart (Figure 2B). The number of slips from the transverse rungs with each forelimb was measured by videotape analysis.[17] A comparison between the control and EE groups was calculated as the difference in the percentage of slips on the transverse rungs of the ladder relative to the total number of steps taken by each forelimb, compared to the control groups.

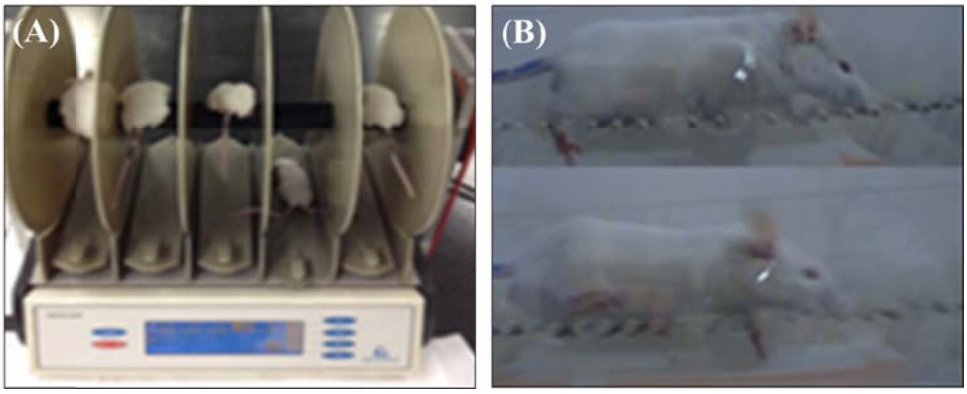

Figure 2. Behavioral tests. (A) Rotarod test. (B) Ladder walking test.

4. RNA preparation

Total RNA was extracted from mouse brain hemispheres using Trizol (Invitrogen Life Technologies, Carlsbad, CA, USA) and purified using RNeasy columns (Qiagen, Valencia, CA, USA) according to the manufacturer' according to the manufacturerumns sbaDNase digestion and clean-up procedures, the RNA samples were quantified, aliquoted, and stored at -80℃ until further use, For quality control, RNA purity and integrity were evaluated by denaturing gel electrophoresis and OD 260/280 ratio and analyzed with an Agilent 2100 Bioanalyzer (Agilent Technologies, Palo Alto, CA, USA).

5. Labeling and purification

Total RNA was amplified and purified using the Ambion Illumina RNA amplification kit (Ambion, Austin, Texas, USA) to yield biotinylated cRNA according to the manufacturer instructions. Briefly, 550 ng of total RNA was

reverse transcribed to cDNA using a T7 oligo (dT) primer. Second strand cDNA was synthesized, transcribed in vitro, and labeled with biotin-NTP. After purification, the cRNA was quantified using an ND-1000 spectrophotometer (NanoDrop, Wilmington, DE, USA).

6. Hybridization and data export

Next, 750 ng of labeled cRNA samples were hybridized to each mouse-8 expression bead array for 16 to 18 hrs at 58 ℃, according to the manufacturer's instructions (Illumina, Inc, San Diego, CA, USA). The detection of array signals was carried out using Amersham Fluorolink streptavidin-Cy3 (GE Healthcare Bio-Sciences, Little Chalfont, UK) following the bead array manual. Arrays were scanned with an Illumina BeadArray Reader confocal scanner according to the manufacturer'Reader confocal

7. Microarray data analysis

The quality of the hybridization and overall chip performance were monitored by visual inspection of both internal quality control checks and the raw scanned data. Raw data were extracted using the software provided by the manufacturer (Illumina Genome Studio v2009.2, Gene Expression Module v1.5.4). Array data were filtered by the detection value of $p < 0.05$ (similar to signal to noise) in at least 50% of the samples (we applied a filtering criterion for data analysis; a higher signal value was required to obtain a detection value of $p < 0.05$). Selected probe signal values were

transformed by the logarithm function and normalized by the quantile method. Comparative analyses between the test group and control group were carried out using the local-pooled-error test and fold change. The false discovery rate was controlled by adjusting *p* values using the Benjamini-Hochberg algorithm. The differentially expressed gene probes were filtered with the adjusted $p < 0.05$ of a local-pooled-error test and with fold change $\geq |2|$. Hierarchical clustering analyses were performed for filtered probes using complete linkage and Euclidean distance as measures of similarity. Biological gene ontology (GO) analysis for the filtered differentially expressed gene probes was performed using PANTHER 6.1 (http://www.pantherdb.org/panther/ontologies.jsp). Fisher exact test was applied to determine the affected pathways.

8. Gene set enrichment analysis

To explore the differentially regulated pathways, we performed GSEA using the microarray data, as described previously, using a GSEA program (http://www.broad.mit.edu/gsea/msigdb/index.jsp).[36-38] This study used C2 curated gene sets (http://www.broadinstitute.org/gsea/msigdb/collections.jsp#C2, version 3), the sizes of which ranged from 10 to 1000 genes. A *p* value < 0.05 was considered significant.

9. Quantitative real-time reverse transcription-polymerase chain reaction (qRT-PCR)

Differentially expressed genes of interest were selected for the validation of the microarray results by qRT-PCR; 1 μg of purified total RNA was used as a template to generate the first strand cDNA using a cDNA kit (Invitrogen Life Technologies, Carlsbad, California). Then, 2 μL of cDNA in a total volume of 20 μL was used in the following reaction. The qRT-PCR was performed in triplicate on a LightCycler 480 (Roche Applied Science, Mannheim, Germany) using the LightCycler 480 SYBR Green master mix (Roche Applied Science, Mannheim, Germany), and the thermocycler conditions were as follows: amplifications were performed starting with a 300sec template preincubation step at 95℃, followed by 45 cycles at 95℃ for 10 sec, 53℃ for 10 sec, and 72℃ for 10 sec. The melting curve analysis began at 95℃ for 5 sec, followed by 1 min at 60℃. The specificity of the produced amplification product was confirmed by the examination of a melting curve analysis and showed a distinct single sharp peak with the expected Tm for all samples. A distinct single peak indicates that a single DNA sequence was amplified during qRT-PCR.

The primers were as follows: mouse Drd1a, 5ted Tm for all samples. A distinct single peak indicates that a single DNA sequence was amplified during thermocycler conditions were as folwere as folhe thermocycler conditions were as folfol was performed using Ppp1r1b, 5′-AGGCCTCTCCACATCAGAGA-3′ and 5′-CCTGGCT GTCTTCTTCTTCG-3′; mouse P2ry12, 5′-GAAGGAGAGCACCCTATGGC-3′ and 5′-AGCACCTCAGCATGCTTGTC-

3llows: moPdyn, 5′-CCATCCCAGAATCCAGAGA A-3′ and 5′-CCAGGGTAGGGTGCATAAGA-3′; mouse GAPDH, 5′-AACTTTGGCATTGTGGAAGG-3′ and 5′-ACACATTGGGGGTAGGAACA-3′. GAPDH (glycerol dehyde 3-phosphate dehydrogenase) was used as the internal control. The expression of each gene of interest was obtained using the $2^{-\Delta\Delta Ct}$ method.

10. Western blotting analysis

To confirm the expression of P2ry12, Drd1a, Slc6a3, Pdyn, and Ppp1r1b levels by long-term exposure to EE or control, 50μg of extracted proteins were dissolved in a sample buffer, boiled for 10 min, and separated on a 10% sodium dodecyl sulfate (SDS) reducing gel. The separated proteins were then equally loaded and transferred onto polyvinylidene difluoride membranes (Amersham Pharmacia Biotech, Little Chalfont, UK) using a transblot system (Bio-Rad, Hercules, California, USA). Blots were blocked for 1 hour in Tris-buffered saline (TBS) containing 5% nonfat dry milk (Bio-Rad, Hercules, California, USA) at room temperature, washed 3 times with TBS, and incubated overnight at 4 nonfat dry milk (Bio-Rad, Hercu: anti-dopamine receptor D1 antibody (DRD1A, 1:1,000; Abcam, Cambridge, UK), anti-DAT antibody (SLC6A3, 1:1,000; Abcam, Cambridge, UK), anti-DARPP-32 antibody (PPP1R1B, 1:1,000; Cell Signaling Technology,

Beverly, MA, USA), anti-P2Y12 antibody (P2RY12, 1:1,000; Abcam, Cambridge, UK), antiprodynorphin (anti-PDYN) antibody (PDYN, 1:1,000; Abcam, Cambridge, UK), and anti-GAPDH antibody (GAPDH, 1:1,000; Cell Signaling Technology, Beverly, MA, USA). The next day, the blots were washed 3 times with TBS plus Tween 20 and incubated for 1 hour with horseradish peroxidaselus Tween 20 and incubated for 1 hour with horseradish peroxidasedaseurcubated for 1 hoantibodies (1:2,000; Santa Cruz, CA, USA) at room temperature. After being washed 3 times with TBS plus Tween 20, the protein was visualized with an enhanced chemiluminescence detection system (Amersham Pharmacia Biotech, Little Chalfont, UK).

Next, to confirm the expression of dopamine receptors such as D1 and D2 receptors by control or EE group (n = 3 each), the striatums were lysed in 500 μl of cold RIPA buffer with protease inhibitor cocktail (Sigma). All steps were performed as mentioned above. The 50 μg of extracted striatal proteins were dissolved in sample buffer (60 mM Tris-HCl, pH 6.8, 14.4 mM β-mercaptoethanol, 25% glycerol, 2% SDS, and 0.1% bromophenol blue), boiled at 70°C for 10 min, and separated on a 4-12% SDS reducing gel. Separated proteins were transferred onto polyvinylidene difluoride membranes (Amersham Pharmacia Biotech, UK) using a trans-blot system (Bio-Rad). Blots were blocked for one hour in Tris-buffered saline (TBS) (10 mM Tris-HCl, pH 7.5, 150 mM NaCl) containing 5% non-fat dry milk (Bio-Rad) at room temperature, washed three times with TBS, and incubated at 4°C overnight with a D1 and D2 receptors (1:1,000, Santa Cruz Biotechnology, CA,

USA) antibodies in TBST (10 mM Tris pH 7.5, 150 mM NaCl, and 0.02% Tween 20) containing 5% non-fat dry milk. The next day, blots were washed three times with TBST and incubated for one hour with horseradish peroxidase-conjugated secondary antibodies (1:2,000, Santa Cruz, CA, USA) at room temperature. After washing three times with TBST, the protein was visualized with an ECL detection system (Amersham Pharmacia Biotech, UK). To confirm the expression of synaptic markers pre-synaptic marker, mouse anti-synaptophysin (1:100, abcam, Cambridge, UK) by EE or control group (n = 3 each). All steps were performed as mentioned above.

11. [^{18}F]FPCIT micro-PET imaging

[^{18}F]FPCIT was synthesized according to the previously described procedure.[39] PET scanning was performed with the Siemens Inveon small animal PET scanner (Siemens Medical Solutions). The scanner has a peak absolute system sensitivity of < 10% for the 250–750 eV energy window, an axial field of view of 12cm and a transaxial field of view of 10 cm.[40] Anesthesia was induced with 2.5% isoflurane and was maintained with 1.5% isoflurane for a 120-min long PET experiment. After administration of [^{18}F]FPCIT (4.71 ± 0.94 MBq), mice were positioned in the center of gantry. Tracer accumulation in the brain was investigated by dynamic PET scans over 120 min after injection of [^{18}F]FPCIT.

PET data were reconstructed in user-defined time frames and lengths (10 sec x 6 frames, 30 sec x 8 frames, 300 sec x 5 frames, 1800 sec x 4 frames) with a voxel size of 0.861386 x 0.861386 x 0.796000 mm by a 2-dimentional order-subset

expectation maximization (OSEM) algorithm (4 iterations and 16 subsets). Image files were evaluated by region-of-interest (ROI) analysis using the software AsiProVM software (Acquisition Sinogram Image Processing software, CTI Concorde Microsystems). ROIs associated with the striatum (Figure 3A) and cerebellum (Figure 3B) were drawn on all coronal brain images, guided by stereotactic coordinates (Figure 3C,D).[41] The decay-corrected time activity curves were presented in units of the standard uptake value (SUV), calculated as (% injected dose/cm^3) x body weight (g) to normalize for the differences in rat weight and administered doses and to compare inter-rat and inter-organ data. All SUV values in the text are the means of the measurements on three mice. Non-displaceable binding potential (BP_{ND}), commonly used as an indication of receptor binding density, is the ratio of the peak values of the specific binding ($SUV_{striatum}$ - $SUV_{cerebellum}$) divided by the non-specific binding ($SUV_{cerebellum}$) at the time of the peak. The cerebellum was used as the reference region because it contains very few dopamine transporters and receptors in adult mice.[42,43] If the computed specific binding was negative, it was given a null value.

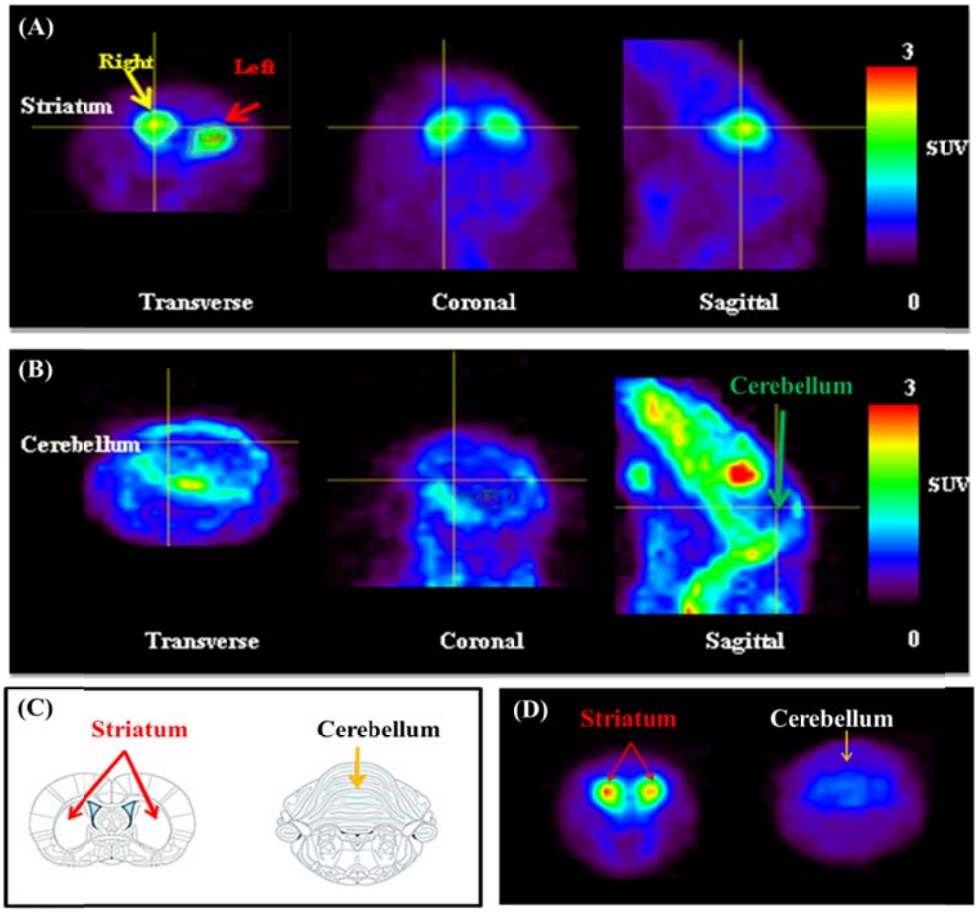

Figure 3. Regions of interest in PET images. (A, B) Brain images were captured striatum region (A) and cerebellum (B). Regions of interest were manually delineated on all brain slices guided by stereotactic templates (C). DAT is predominantly located in the striatum. The cerebellum was used as the reference region because it contains very few dopamine transporters (D).

12. DAT inhibitor treatment

The BZT analogue, JHW007 [(N-(n-butyl)-3α-[bis(4′-fluorophenyl) methoxy]-tropane); Tocris, Bristol, UK], was synthesized as described previously.[44,45] The purity of the compound was analyzed by magnetic resonance, which exceeded 98%. JHW007 was dissolved in 0.9% saline and sonicated until complete solubilization was achieved. It was then injected at doses of 15 mg/kg i.p. for 2 mo.

13. Surface biotinylation assay

In the present study, Sulfo-NHS-biotin (Thermo, MA, USA) was used to isolate plasma membrane-associated DAT protein prepared from the striatum region of the EE or control conditioned mice. DAT protein was subsequently identified by immunoreactivity using a DAT antibody. Larger amounts of striatal protein (400 μg) were used to determine NHS-biotin-labeled cell surface DAT.[31] Chopped striatum proteins were washed with ice-cold PBS containing 1 mM $MgCl_2$ and 0.1 mM $CaCl_2$ (PBS^{++}) and incubated with 1 mg/ml EZ-link Sulfo-NHS-SS-Biotin (Thermo, MA, USA) in PBS^{++} for 1 hr at 4°C with gentle shacking. The reaction was quenched by washing with 0.1% BSA in 4°C PBS^{++}. The cells were lysed with 100 μl cold RIPA buffer (50 mM Tris-HCl, pH 7.5, 1% Triton X-100, 150 mM NaCl, 0.1% sodium dodecyl sulfate (SDS), 1% sodium deoxycholate with a protease inhibitor cocktail (Sigma, Darmstadt, Germany). Protein lysates were then centrifuged at 13000 rpm at 4°C for 20 min. The supernatant was extracted, and incubated with NeutrAvidin agarose resin (Pierce, MA, USA) for 2 hr at 4°C. The

resin was washed and the bound proteins were eluted by mixing and incubating with 2X SDS sample buffer at 70°C for 10 min. The eluted sample was analysed by Western blotting.

14. *In Situ* proximity ligation assay

The Duolink® kit (Olink Bioscience, Uppsala, Sweden) is based on the use of two unique and bi-functional probes called PLA™. Each probe consists of a secondary antibody attached to a unique synthetic oligonucleotide that acts as a reporter. After exposure for 8 wks to the EE or control condition, the striatum region was stained with DAT and phosphoserine primary antibodies over-night at 4°C to detect interacting DAT and phosphoserine proteins. After washing, the sections were incubated with the secondary oligonucleotide-linked antibodies (PLA probes) provided in the kit. The oligonucleotides bound to the antibodies were hybridized, ligated, amplified, and detected using a fluorescent probe (Detection Kit 563).[46] Dots were detected by confocal imaging (LSM700, Zeiss, Oberkochen, Germany).

15. Immunoprecipitation

To identify DAT and its phosphorylation regulated by EE, the striatums were lysed in 500 μl of cold RIPA buffer (50 mM Tris-HCl, pH 7.5, 1% Triton X-100, 150 mM NaCl, 0.1% sodium dodecyl sulfate (SDS), 1% sodium deoxycholate) with protease inhibitor cocktail (Sigma, Darmstadt, Germany). Tissue lysates were then centrifuged at 13000 rpm at 4°C for 20 min, the supernatant was extracted and protein concentrations were measured using the Bradford method. For co-

immunoprecipitation experiments, solubilized specific brain regions extracts (1,000 μg of protein) were incubated in the presence of primary anti-DAT antibodies (1:500; Chemicon) for 24 h at 4°C, followed by the addition of 20 μl of protein A/G agarose (Santa Cruz Biotechnology) for 3 h at 4°C. Then the solubilized specific brain regions extracts with the primary anti-DAT antibodies and protein A/G agarose were centrifuged at 3000 rpm at 4°C for 1 min. Beads were washed four times in the buffer described above, boiled for 5 min in SDS sample buffer, and subjected to Western blot for anti-DAT and anti-phosphoserine. The proteins were visualized with enhanced chemiluminescence reagents as described (Amersham Biosciences, Little Chalfont, UK).

To confirm the expression of PKC by control or EE group (n = 3 each), the striatum was lysed in 500 μl of cold RIPA buffer with protease inhibitor cocktail (Sigma). All steps were performed as mentioned above. After IP and transfer onto a membrane, Western blot analysis was used to detect expression of anti-PKCβI (1:1,000, Santa Cruz Biotechnology).[47] In addition, to validate that the DAT inhibition occurs via phosphorylation mechanism, SH-SY5Y neuroblastoma cells were treated with the DAT inhibitor (JHW007 15 μg/ml) for 2 min at 37°C.[48] Cells Larger amounts of cells protein (200 μg) were used to identify DAT and its phosphorylation regulated by DAT inhibitor using immunoprecipitation.

16. Immunohistochemistry for location of DAT in striatum

At 8 wks post-treatment, mice were deeply anaesthetized and perfused transcardially with 4% paraformaldehyde in 0.1 M phosphate buffer, pH 7.4. The

animals were anesthetized with a mixture of Ketamine (100 mg/kg, Huons, Gyeonggi-do, South Korea) and Rumpun (10 mg/kg, Bayer Korea, Gyeonggi-do, South Korea). Brains were removed and post-fixed 1h, followed by cryoprotection in 30% sucrose in Tris-buffered saline containing 0.02% sodium azide. Immunohistochemistry (IHC) was performed at post-treatment 8 wks. The brain tissues were frozen and cryosectioned at 16 μm intervals. To confirm location of dopamine transporter, the brain sections of the striatum were immunostained with the DAT marker, rat anti-DAT (1:400, chemicon, Pemecula, CA) and pre-synaptic marker, mouse anti-synaptophysin (1:100, abcam, Cambridge, UK) or post-synaptic marker, rabbit anti-PSD95 (1:400, abcam, Cambridge, UK). Double-labeled DAT^+/$synaptophysin^+$ cells or DAT^+/$PSD\text{-}95^+$ cells were then assessed by confocal imaging (LSM700, Zeiss, Gottingen, Germany).

17. Statistical analysis

All statistical analyses were performed with SPSS Statistics 18.0 (IBM Corp., Armonk, NY, USA), and all data are expressed as mean ± SEM. To compare continuous variables between groups, independent t-test and one-way ANOVA followed by post-hoc multiple comparison with Bonferroni test were used. A p value < 0.05 was considered statistically significant.

III. RESULTS

1. The rotarod test showed that EE improved locomotor function

Six-week old CD-1 (ICR) mice were randomly allocated to either EE or standard conditions for 2 mo (n = 10 per group) (Figure 1). To determine whether EE exposure improves motor function, rotarod tests were performed with accelerating (4-80 rpm) and constant (64 rpm) paradigms every 2 wks. In the pretreatment evaluation, no statistical differences were seen between the groups. EE-induced improvement of rotarod performance relative to controls was significantly evident at 2 wks post-treatment. A significant improvement was observed starting at 2 wks post-treatment for the accelerating speed condition (192.4 ± 15.1 in EE and 109.9 ± 13.3 s in control, $t = 4.104$, $p < 0.05$; Figure 4A) and for the constant speed condition (50.6 ± 20.1 in EE and 7.8 ± 1.9 s in control, $t = 2.115$, $p < 0.05$; Figure 4B). This improved motor function was maintained throughout the study period. Finally, 8 wks after the treatment, the mean rotarod latencies of the EE mice increased significantly to 182.7 ± 17.9 s for the accelerating speed condition ($t = 3.949$, $p < 0.05$; Figure 4A) and to 122.4 ± 32.0 s for the constant-speed condition ($t = 3.441$, $p < 0.05$; Figure 4B), compared with the rotarod latencies of the control mice (102.6 ± 9.6 and 11.7 ± 3.3 s, respectively).

2. Ladder walking test showed improvement of fine motor function by EE

To assess fine motor function more thoroughly between the EE and control groups (n=10 each), ladder walking tests were performed at pre-treatment and 8 wks after

EE (Figure 4C). In the ladder walking test, the percentage of slips on the transverse rungs of the ladder relative to the total number of steps by the right and left forelimbs were significantly decreased only in the EE mice (0.5 ± 0.2% and 0.2 ± 0.1%, respectively) compared with the forelimb slip rate (%) of the control mice (1.4 ± 0.3% and 1.8 ± 0.4%, respectively) at 8 wks post-treatment ($t = 2.528$, $p < 0.05$ in the right forelimb and $t = 3.995$, $p < 0.05$ in the left forelimb). Taken together, results in both the rotarod test and the ladder walking test suggest that EE can improve motor function.

(A)

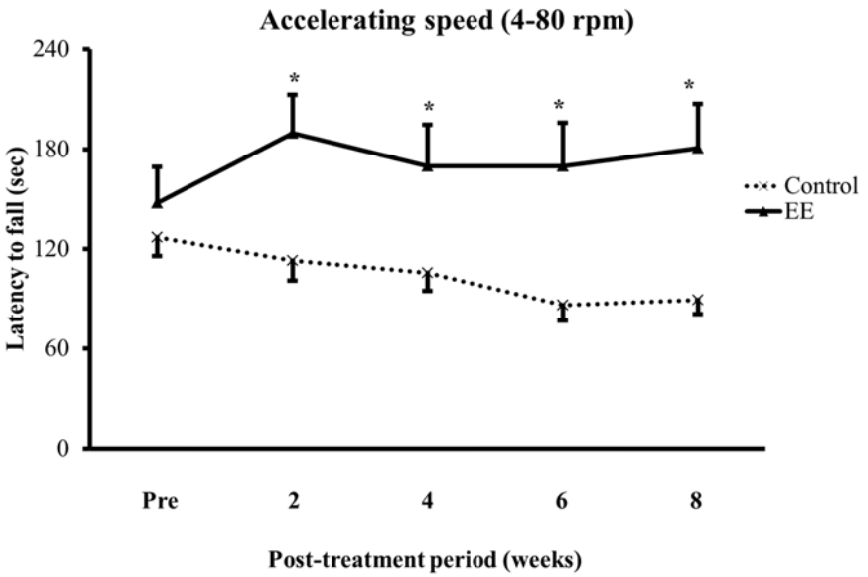

(B)

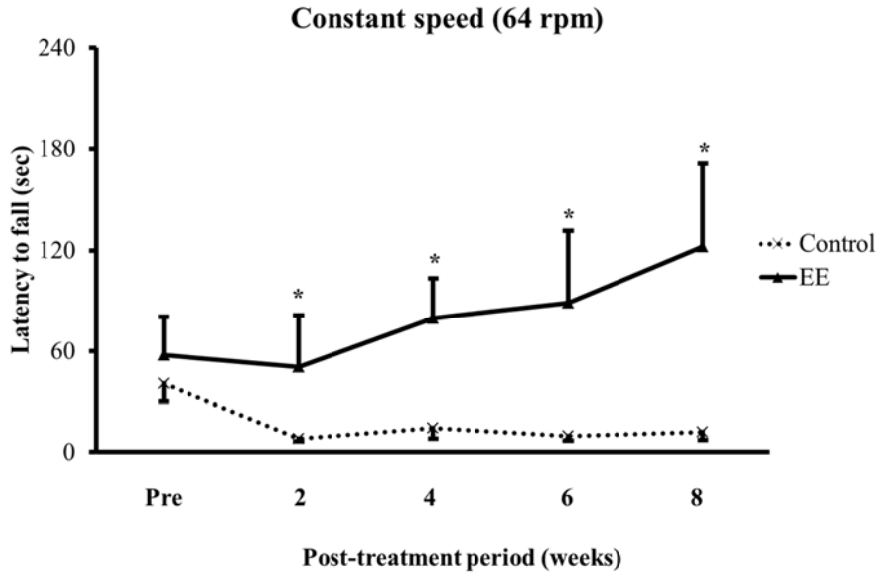

(C)

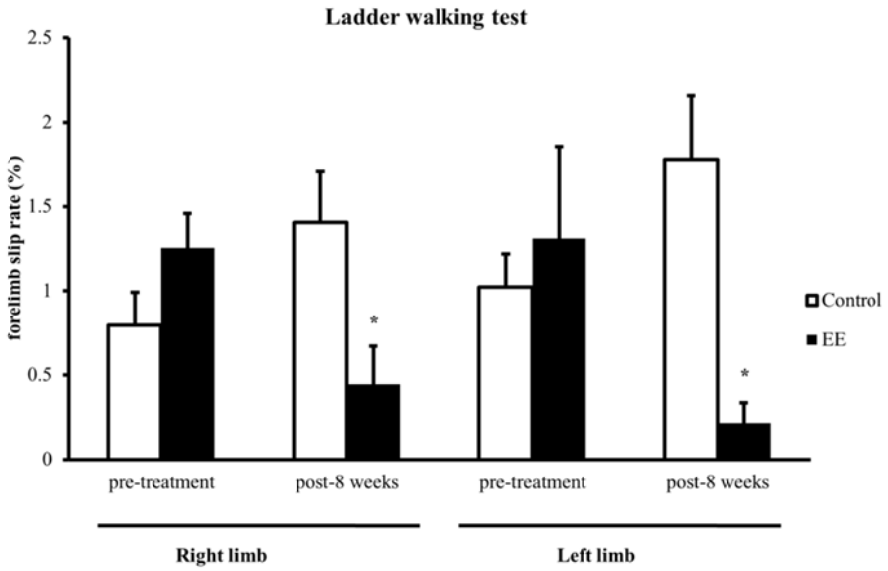

Figure 4. Improved motor functions after exposure to EE. (A) For the accelerating speed (4-80 rpm) rotarod test, a significant improvement was observed starting 2 wks after the exposure to EE. At 8 wks post-treatment, the mean rotarod latency of the EE mice was significantly higher than the latency of control mice. (B) For the constant speed (64 rpm) rotarod test, a significant improvement was also observed starting 2 wks after exposure to EE. At 8 wks post-treatment, the mean rotarod latency of the EE mice was significantly higher than the latency of control mice. (C) In the ladder walking test, EE mice also showed a significant reduction in the percentage of the total slips among total steps with both forelimbs at 8 wks post-treatment.

3. Microarray data revealed global changes in gene expression patterns in the brain of mice exposed to EE

To investigate the underlying mechanisms associated with EE-induced behavioral improvement, this study performed microarray analyses of total RNA extracts from mouse brain hemispheres. Hierarchical clustering using the significantly regulated genes showed that the gene expression patterns were similar among samples within the same group but were more than 2-fold difference between the groups (Figure 5A). Hierarchical clustering analysis showed that the gene expressions in the EE group were distinct from those of the control group in that 17 genes were significantly upregulated and 31 genes were significantly downregulated by more than 2-fold in the EE group compared with the control group ($p < 0.05$; Figure 5B). To analyze further differences in gene expression between the groups, next categorized genes exhibited significantly altered expression levels after exposure to EE according to their biological functions. The analysis using the GO database revealed that the expression levels of 11 genes involved in signal transduction; 9 genes in nucleoside, nucleotide, and nucleic acid metabolism; 9 genes in developmental processes; 8 genes in neuronal activities; and 6 genes in transport pathways were significantly altered after exposure to EE (Figure 5C). To determine the statistical significance of these changes, this study performed Fisher's exact test. "Neuronal activities" was the only category shown to be statistically regulated by EE ($p < 0.05$; Table 1), suggesting that EE may preferentially regulate neuronal activity genes in brain tissue. Furthermore, 8 genes involved in neuronal activities were found to be differentially regulated. Among these genes, there were significant

increases in Drd1 (dopamine receptor D1A, 2.3-fold), Pdyn (PDYN, 2.6-fold), Ppp1r1b (protein phosphatase 1, regulatory subunit 1B, 2.1-fold), and P2ry12 (purinergic receptor P2Y, G protein-coupled 12, 2.9-fold) after EE exposure. In contrast, drastic decreases were observed in Slc6a3 (DAT, 7.4-fold) as well as Slc6a4 (serotonin transporter, 3.8-fold) after EE exposure, raising the possibility that the presynaptic reuptake of these neurotransmitters might be reduced by long-term exposure to EE.

(A)

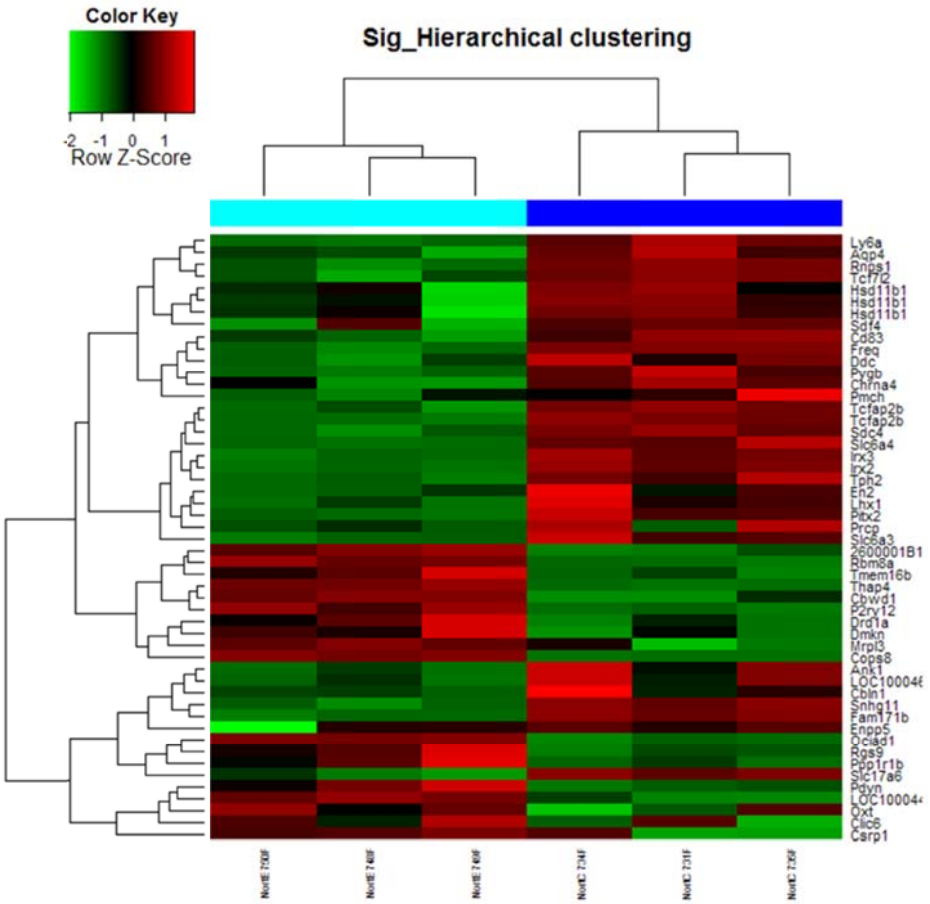

(B)

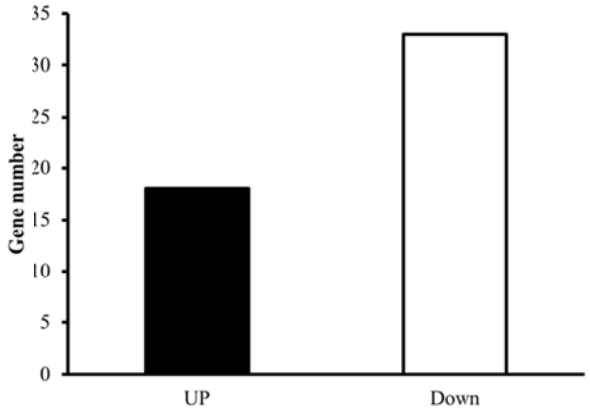

(C)

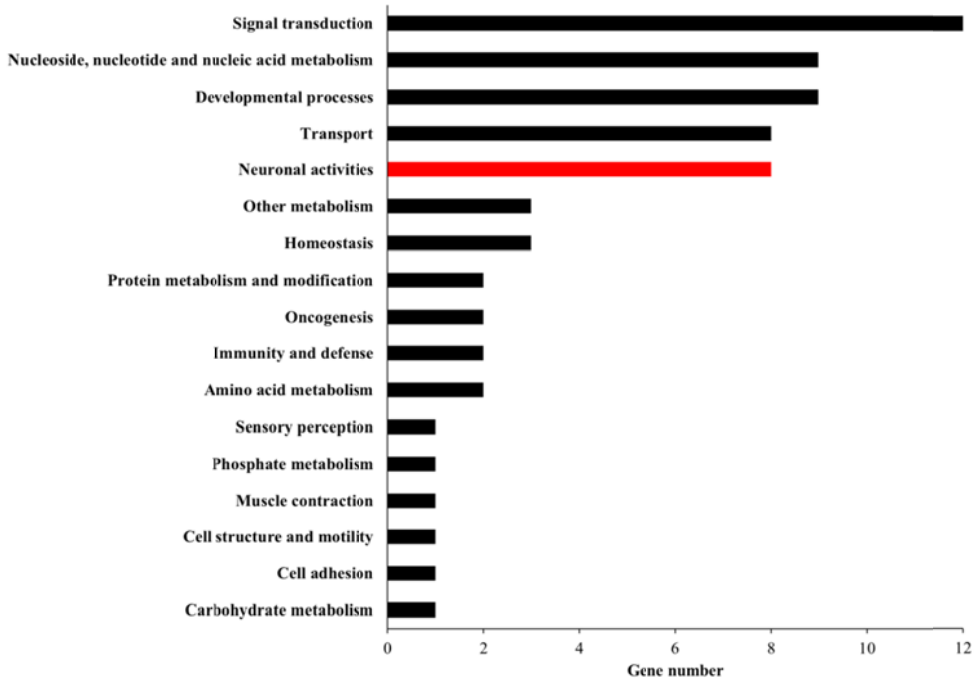

Figure 5. Microarray data reveals the global change of gene expression patterns in the brain of mice exposed to EE. Genes that demonstrated significantly different expression levels between EE and Control groups by more than 2-folds were regarded as significantly regulated genes and used for further analysis ($p < 0.05$). (A) Hierarchical clustering using the significantly regulated genes showed that gene expression patterns were similar among samples within the same group, but different between the groups (more than 2 folds). (B) The number of up- or downregulated genes differed in the intact brain hemispheres following environmental enrichment. (C) The significantly regulated genes were categorized into gene sets, which was pre-determined based on the function of the genes.

Table 1. Genes significantly different between EE and control groups as classified by biological function.[a]

Biological Process	Total Probes (No.)	Number	*p* Value
Carbohydrate metabolism	383	1	1.00
Cell adhesion	337	1	1.00
Cell structure and motility	744	1	1.00
Muscle contraction	114	1	1.00
Phosphate metabolism	68	1	1.00
Sensory perception	202	1	1.00
Amino acid metabolism	161	2	0.48
Immunity and defense	766	2	0.96
Oncogenesis	245	2	0.63
Protein metabolism and modification	1997	2	1.00
Homeostasis	132	3	0.10
Other metabolism	391	3	0.47
Neuronal activities	484	8	0.00
Transport	929	8	0.08
Developmental processes	1332	9	0.16
Nucleoside, nucleotide, and nucleic acid metabolism	2188	9	0.67
Singal transduction	2540	12	0.45

Abbreviations: EE, enriched environment
a.The probes were classified into 17 categories based on the biological functions of the corresponding genes and the number of probes for differentially regulated expression levels between the EE and control groups with $p < 0.05$ and $|\text{fold change}| > 2$.

4. GSEA showed genes involved in synaptic plasticity are regulated by long-term exposure to EE

To determine more thoroughly the pathways selectively regulated by exposure to EE compared with the control cages, this study adopted GSEA as previously described.[36-38] GSEA allowed us to determine the selectively regulated pathways among 3,272 gene sets, whereas the GO analysis this study performed used only 17 categories. Compatible with the GO analysis results, GSEA revealed that several pathways associated with synaptic plasticity were significantly altered by EE exposure (Figure 6). GSEA showed that the gene sets involved in synaptic plasticity were regulated by exposure to EE. Namely, genes associated with transmission across chemical synapses, opioid signaling, neurotransmitter receptor binding and downstream transmission in the postsynaptic cells, G protein activation, kainate receptor activation, and depolarization of the presynaptic terminal triggering the opening of calcium channels and the acetylcholine release cycle were upregulated, whereas those linked with dopamine neurotransmitter release and Na^+/Cl^--dependent transporters were downregulated.

The global expression levels of genes associated with the transmission of neurotransmitters across chemical synapses were significantly higher in the EE group compared with the control group, suggesting that EE may activate the transfer of information across chemical synapses (Figure 6A; $p < 0.05$). In agreement with this, genes involved in opioid signaling were globally upregulated in the EE group, implying that EE can activate opioid signaling (Figure 6B; $p < 0.05$). This GSEA result of opioid signaling is compatible with previous reports that showed, based on

biochemical and functional analyses, that exercise activates opioid production and signaling.[49-51] In line with this enhanced transmission across chemical synapses, genes involved in neurotransmitter receptor binding and downstream transmission in postsynaptic cells as well as G protein activation were globally upregulated (Figures 6C and 6D; $p < 0.05$), suggesting that EE exposure may increase postsynaptic sensitivity. Compatible with this general postsynaptic receptor activation by EE, the global expression levels of genes involved in kainate receptor activation were significantly higher in the EE group than in the controls (Figure 6E; $p < 0.05$), suggesting that EE may activate non-NMDA (N-methyl D-aspartate) glutamate receptors as well.

Although EE exposure consistently upregulated genes related to transmission across synapses and postsynaptic receptor activation, genes involved in neurotransmitter release did not show uniform change after long-term exposure to EE. Genes involved in the depolarization of presynaptic terminal triggering, for example, the opening of the calcium channel, were significantly, but only marginally, upregulated in the EE group compared with the controls (Figure 6F; $p < 0.05$), suggesting that EE exposure may activate the release of some neurotransmitters from presynaptic terminals. Genes associated with acetylcholine and dopamine release were significantly upregulated and downregulated, respectively (Figure 6G-H, $p < 0.05$), suggesting that EE can increase acetylcholine release and reduce dopamine release after long-term exposure to it.

It is interesting to note that genes associated with Na^+/Cl^--dependent transporters were globally downregulated in the EE group compared with the controls (Figure 6I;

$p < 0.05$). Given that the activity of a neurotransmitter is terminated by reuptake at presynaptic neurons, the downregulation of genes associated with Na^+/Cl^--dependent transporters can enhance the activity of neurotransmitters at the synaptic level. Leading-edge analysis showed that this global downregulation of Na^+/Cl^--dependent transporters was associated with the selective downregulation of 7 genes, especially Slc6a3, which is responsible for the presynaptic reuptake of dopamine (Figure 6J). The Slc6a3 gene was also downregulated in the microarray results. Taken together, the GSEA results suggested that EE may enhance synaptic activity by increasing postsynaptic sensitivity and reducing presynaptic neurotransmitter reuptake.

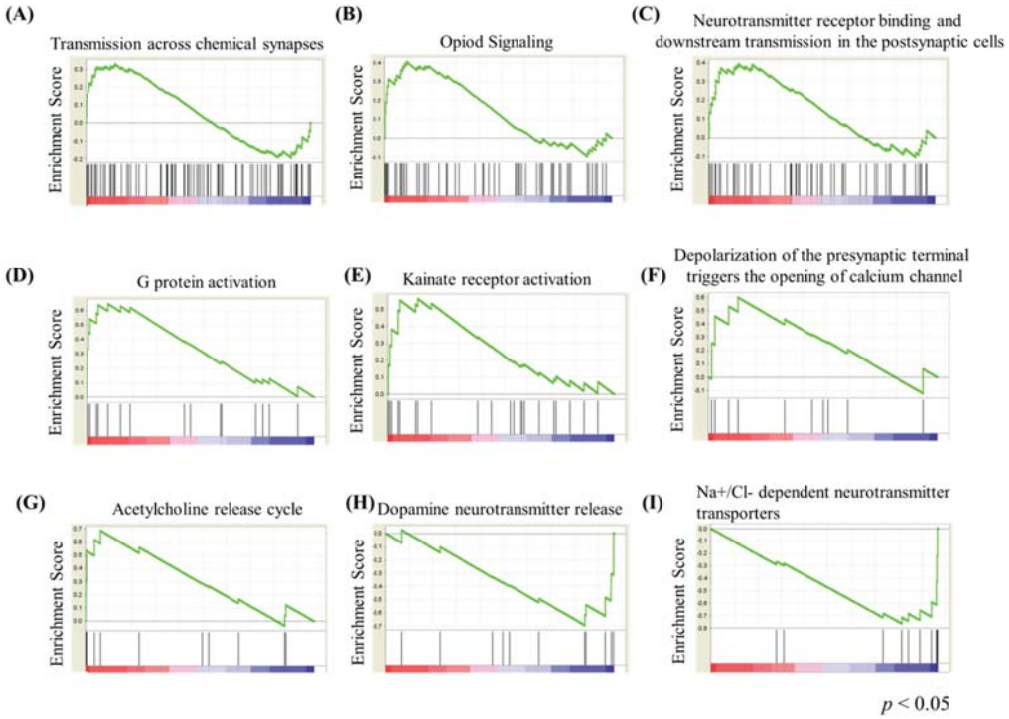

(J)

Gene symbol	Gene description
SLC6A1	solute carrier family 6 (neurotransmitter transporter, GABA), member 1
SLC6A19	solute carrier family 6 (neutral amino acid transporter), member 19
SLC6A15	solute carrier family 6, member 15
SLC6A7	**solute carrier family 6 (neurotransmitter transporter, L-proline), member 7**
SLC6A6	**solute carrier family 6 (neurotransmitter transporter, taurine), member 6**
SLC6A13	**solute carrier family 6 (neurotransmitter transporter, GABA), member 13**
SLC6A9	**solute carrier family 6 (neurotransmitter transporter, glycine), member 9**
SLC6A3	**solute carrier family 6 (neurotransmitter transporter, dopamine), member 3**
SLC6A12	**solute carrier family 6 (neurotransmitter transporter, betaine/GABA), member 12**
SLC6A11	**solute carrier family 6 (neurotransmitter transporter, GABA), member 11**

Figure 6. GSEA shows genes involved in synaptic plasticity are regulated by exposure to EE. (A-G) GSEA shows significantly upregulated gene sets in EE groups compared to control. (H-I) GSEA shows significantly downregulated gene sets in EE compared to control. (J) Leading edge analysis of "Na^+/Cl^- dependent neurotransmitter transporters" gene sets shows that seven genes (highlighted in yellow), including Slc6a3, comprise the leading edge responsible for the global downregulation of the gene set of Na^+/Cl^- dependent neurotransmitter transporters. GSEA: Gene set enrichment analysis (GSEA).

5. Validation of microarray data using qRT-PCR and western blotting

To validate the microarray data, qRT-PCR and western blotting were used in this study. This study performed qRT-PCR on the genes that had a significant change of more than 2-fold in the microarray and found that the RT-PCR data were compatible with those from the microarray (Figure 7A). The qRT-PCR confirmed that dopamine D1 receptor Drd1a, protein phosphatase 1 regulatory subunit 1B Ppp1r1b, and endogenous opioid peptide Pdyn significantly increased after long-term exposure to EE, whereas Na^+/Cl^- -dependent neurotransmitter transporters Slc6a3 and Slc6a4 significantly decreased in a similar pattern to the microarray data (Figure 7A).

This study next determined the protein levels of these genes (Drd1a, Slc6a3, Ppp1r1b, P2ry12, and Pdyn) in specific regions of the brain such as the frontal cortex, basal ganglia, and hippocampus (Figure 7B). Western blotting showed that dopamine receptor DRD1A protein increased in the basal ganglia, whereas dopamine transporter SLC6A3 protein decreased in the basal ganglia after exposure to EE. It is important that cAMP-regulated neuronal phosphoprotein DARPP32, encoded by the Ppp1r1b gene, drastically increased in brain regions including the frontal cortex, basal ganglia, and hippocampus by sustained exposure to EE. The protein level of G protein-coupled purinergic receptor P2RY12 increased in the hippocampus after long-term exposure to EE. The endogenous opioid peptide PDYN increased in the cerebral hemisphere, although this increase was not significant in the regional analysis.

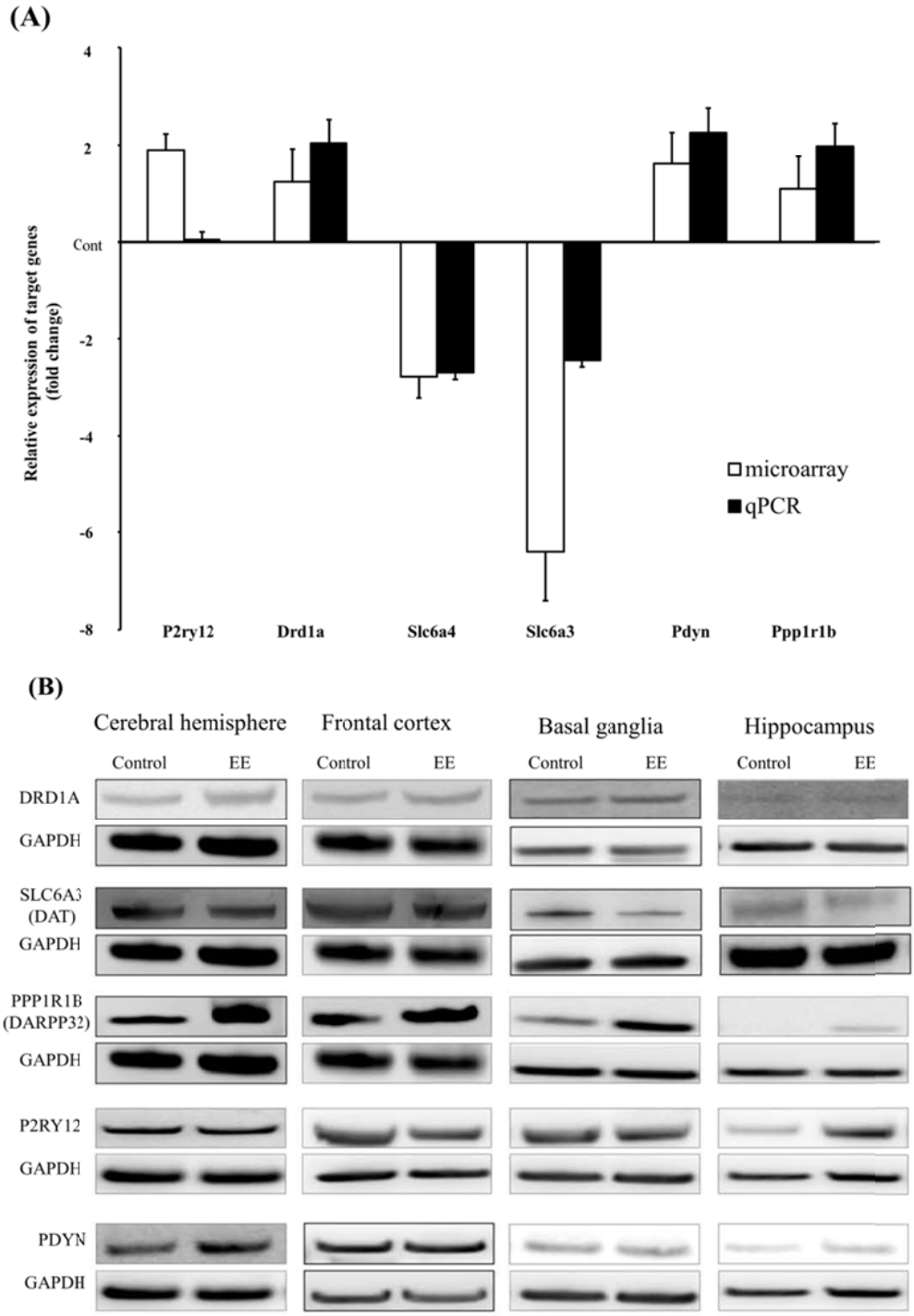

Figure 7. Validation of microarray results by quantitative real-time reverse transcription-polymerase chain reaction (qRT-PCR) and Western blotting: Total RNA (A) and protein (B) were isolated from the brains of mice after an 8-week exposure to either EE or control and were subjected to qRT-PCR (A) or Western blotting on those genes with a significant change of more than 2-fold in the microarray. (A). The qRT-PCR confirmed that Drd1a, Ppp1r1b, Pdyn significantly increased after long-term exposure to EE, whereas Na^+/Cl^--dependent neurotransmitter transporters Slc6a3 and Slc6a4 significantly decreased in a similar pattern to the microarray data. (B). Western blotting showed that dopamine receptor DRD1A protein increased in the BG, whereas DAT SLC6A3 protein decreased in the basal ganglia after exposure to EE. In addition, cAMP-regulated neuronal phosphoprotein, DARPP32 (PPP1R1B) increased in all brain regions analyzed. The protein level of G protein-coupled purinergic receptor P2RY12 increased in the hippocampus after long-term exposure to EE.

6. PET image assay showed that EE down-regulated striatal DAT

This study was performed a [^{18}F]FPCIT PET scan in the mouse brain after EE to investigate changes of DAT expression. DAT was mainly expressed in the striatal region, but the cerebellum has little DAT expression. Therefore, the expression of the cerebellum was used as a negative control. In the time activity curves, cerebellar uptakes between EE and control group were similar. However, the striatal uptake of EE was lower than that of the control group (Figure 8A). Representative brain PET images were captured between 22-45 min, and combined to generate the averaged images (Figure 8B) of each EE and control. Binding values of striatal DAT were significantly decreased approximately 18% in the EE mice (2.7 ± 0.05 BP_{ND}) relative to the control mice (3.3 ± 0.2 BP_{ND}) at 8 wks post-treatment (t = 2.28, p < 0.05; Figure 8C).

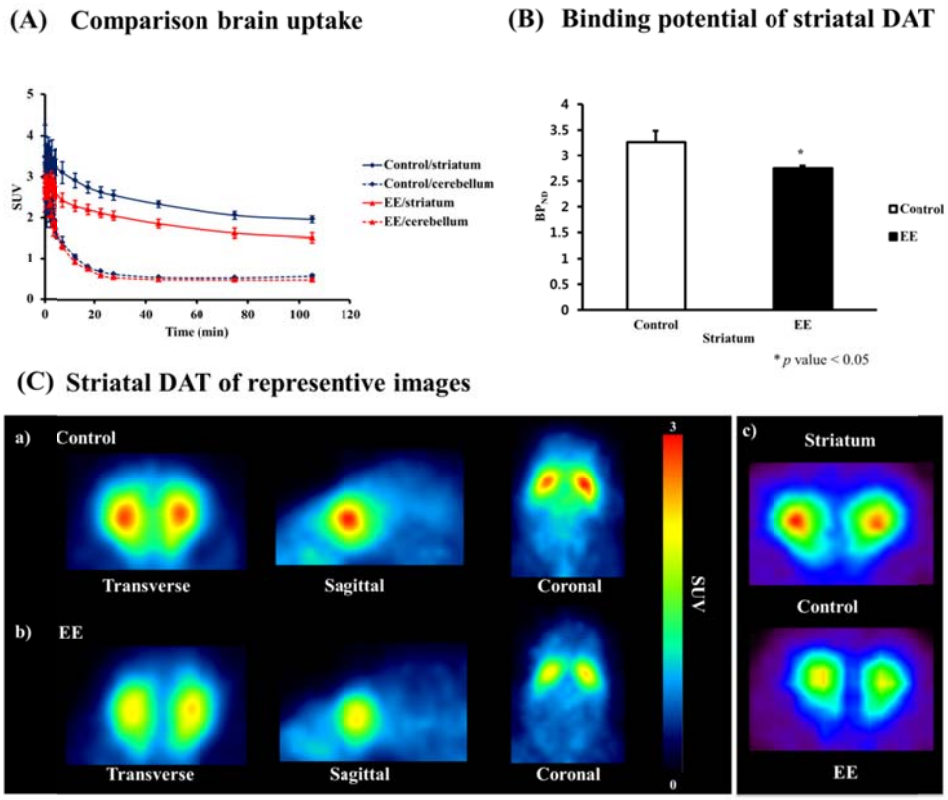

Figure 8. EE mediated down-regulation of DAT in the striatum. (A) Time activity curves in the specific brain regions for EE and control groups. Whereas radioactivities in the cerebellum were similar each other, striatal uptake in EE mice was lower than that in control group. (B) Binding values of striatal DAT were significantly decreased approximately 18% in the EE mice relative to the control mice at 8 week post-treatment. (C) Brain images were captured between 22-45 min and combined to generate the averaged images in control a) and EE mice b) Representative brain PET image in EE indicated decreased uptake of the DAT in the striatal region c).

7. Surface biotinylation assay showed that EE induced DAT internalization

This study considered that these patterns of decreased DAT in PET occurred due to internalization after EE. In order to confirm DAT internalization, this study performed a biotinylation assay for striatal membrane DAT. EE significantly decreased the membrane DAT (0.7 ± 0.1 folds), which was approximately 30% lower than that of the control groups (1.0 ± 0.04 folds) at 8 wks post-treatment (t = 2.930, $p < 0.05$; Figure 9A), suggesting that a membrane DAT is internalized to the intracellular region of the striatum after exposure to EE.

8. DAT phosphorylation increased after exposure to EE

To investigate DAT internalization by post-translational modification, this study evaluated the phosphorylation level of DAT since DAT phosphorylation plays a role in DAT recycling and transporter internalization.[52] In order to confirm phosphorylation of DAT in the striatal region the interaction between endogenous DAT and phosphoserine was examined by an *in situ* proximity ligation assay, which enables visualization of the protein-protein interaction in close proximity (< 40 nm) through ligation-mediated amplification of a specific oligonucleotide probe. After exposure to EE, fluorescent signal area of DAT phosphorylation significantly increased in the striatum compared with the control group (t = 3,180, $p < 0.05$; Figure 9B).

Then this study performed an immunoprecipitation (IP) assay using anti-DAT and anti-phosphoserine antibodies to confirm DAT phosphorylation by EE. After exposure to EE, DAT phosphorylation significantly increased in the striatum (1.5 ±

0.1 folds) relative to the control group (1.0 ± 0.1 folds) (t = 4.073, p < 0.05; Figure 9C), suggesting that DAT internalization occurred by phosphorylation. In addition, this study investigated the interaction between DAT and PKC using IP to study whether DAT phosphorylation is controlled by PKC. This study confirmed that DAT is bound with PKC, and the PKC levels increased in the striatum after exposure to EE (1.3 ± 0.1 folds) relative to the control group (1.0 ± 0.1 folds) (t = 2.464, p < 0.05, Figure 9C). Taken together, this study suggests that EE enables phosphorylation of DAT via the PKC-mediated pathway in the striatum.

(A) Biotinylation assay

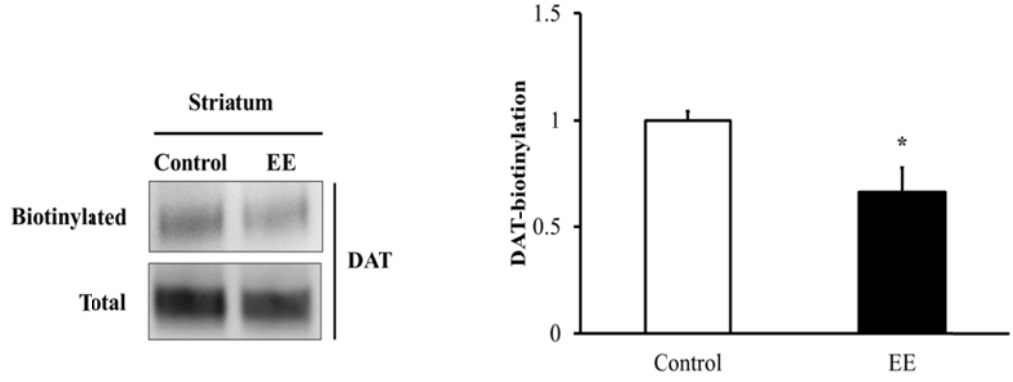

*p value < 0.05

(B) *In situ* PLA assay

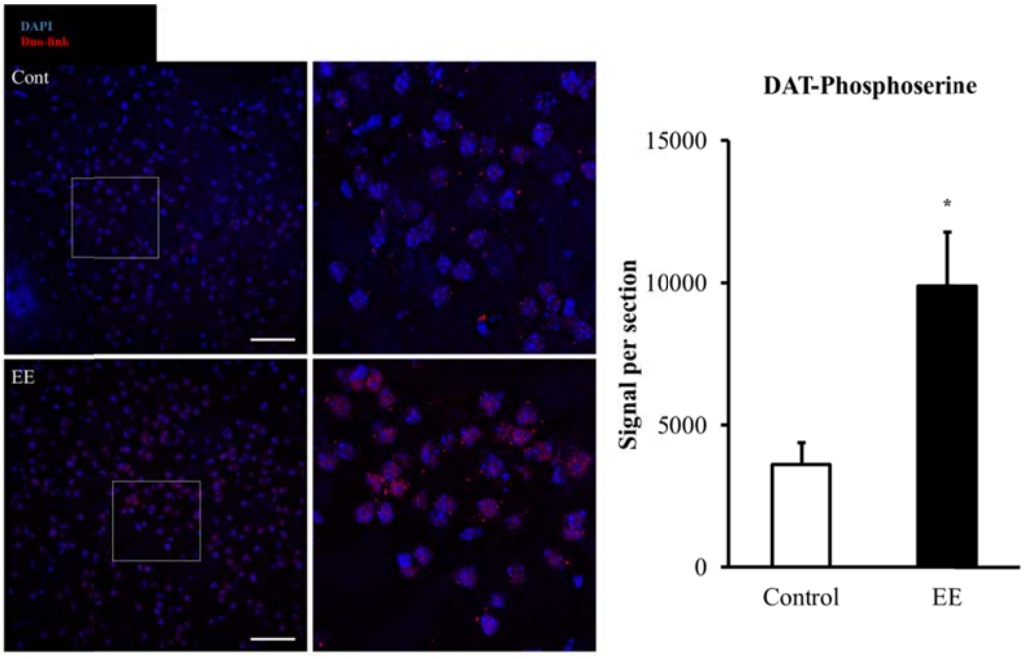

Scale bar = 50 μm

*p value < 0.05

(C) IP assay

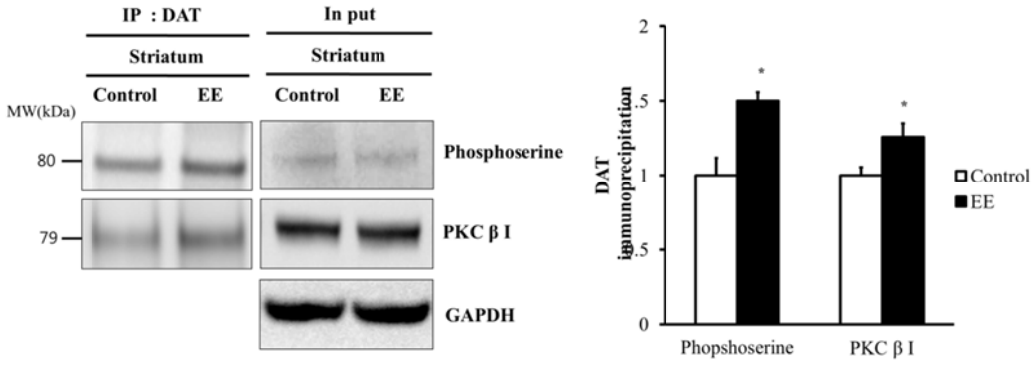

*p value < 0.05

Figure 9. Internalization and phosphorylation of striatal DAT induced by EE. (A) Internalization of striatal membrane DAT by a surface biotinylation assay. After exposure to EE, membrane DAT significantly decreased compared with the control group at 8 wks post-treatment. (B) *In situ* proximity ligation assay for phosphorylation of DAT. The red color indicates the phosphorylation states showing increased fluorescent signal area of the DAT phosphorylation in the striatum after exposure to EE. The scale bar indicates 50 μm. (C) Immunoprecipitation (IP) for phosphorylation of DAT and for interaction between DAT and PKC. The levels of the DAT phosphorylation and the PKCβ bound with DAT significantly increased in the striatum after exposure to EE. Western blot of inputs for the immunoprecipitation reactions was shown in (C)

9. Decreased DAT is not associated with the increment of dopamine D1 and D2 receptors in EE

This study performed western blotting to analyze expression of dopamine D1 and D2 receptors in striatum by EE exposure. This result did not show that decreased DAT is associated with the increment of dopamine D1 and D2 receptors in EE (Figure 10). Previous studies demonstrated that there was no evidence that EE influenced D2 receptor density, or the ratio of D2 receptor density to other receptor types[39] and destruction of DAT in Parkinson's animal model did not show statistically significant increment of D2 receptors.[40]

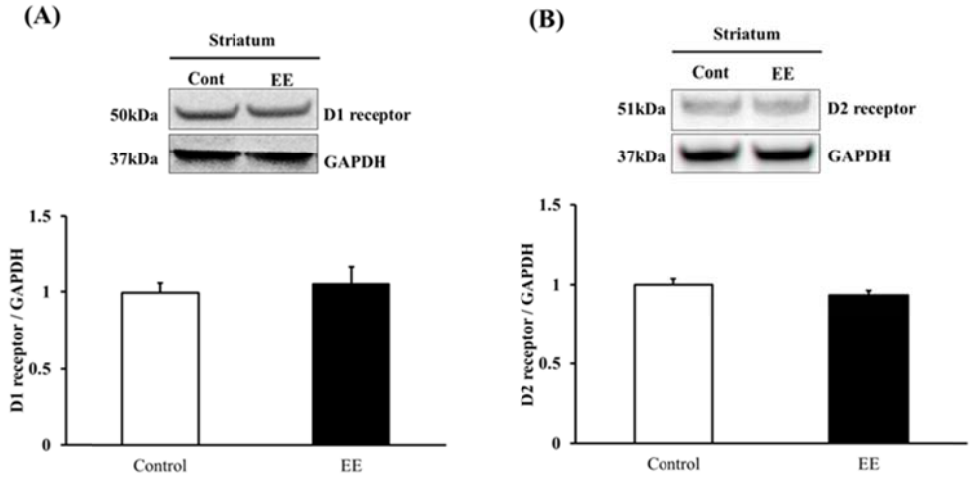

Figure 10. Expression of dopamine D1 and D2 receptors in the striatum. (A) The levels of the dopamine D1 receptor in EE had no difference with control group in the striatum. (B) Western blotting analysis confirmed the levels of the dopamine D2 receptor in EE, showing the level of the dopamine D2 receptor in EE had no difference with control group.

10. DAT inhibitor treatment improved motor function and increased DAT phosphorylation

To determine whether DAT inhibitor, JHW007, treated groups showed improvement on motor function, rotarod tests were performed with accelerating paradigms (4-80 rpm) 8 wks after treatment with either JHW007 or saline in the EE and control mice (n = 5 per group). In the pretreatment evaluation, no statistical differences were seen between the groups. EE and JHW007 treatment (196.8 ± 30.0 s in the saline-treated EE mice, 176.9 ± 25.5 s in the JHW007-treated EE mice, and 176.5 ± 33.8 s in the JHW007-treated control mice) resulted in significantly improved rotarod performance relative to the saline-treated controls (88.1 ± 21.0 s) at 8 wks post-treatment ($F = 3.073$, $p < 0.05$; Figure 11A). When this study also validated the DAT inhibition occurred via phosphorylation mechanism with *in vitro* experiment, DAT inhibitor treatment showed DAT phosphorylation significantly increased in SH-SY5Y cells (1.6 ± 0.1 folds) relative to the control ($t = 3.357$, , $p < 0.05$; Figure 11B).

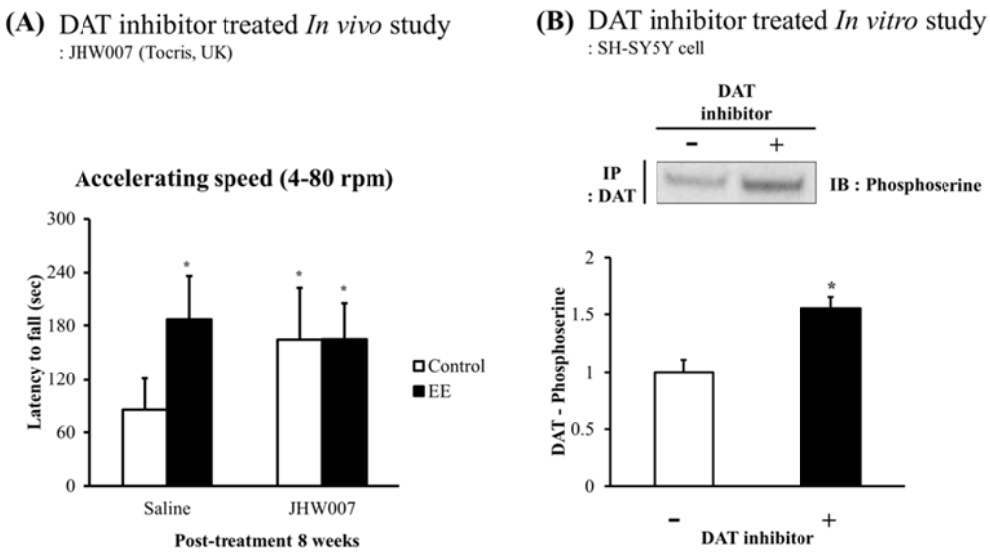

Figure 11. DAT inhibitor recapitulated EE-mediated treatment benefits and phosphorylation of DAT induced by DAT inhibitor in vitro (A) The effect of a DAT inhibitor, JHW007. Rotarod tests were performed with accelerating (4-80 rpm) paradigms 8 wks after exposure on either mice from the JHW007-treated EE and control groups or the saline-treated EE and control groups (n = 5 per group). In the pretreatment evaluation, no statistical differences were seen between the groups. At 8 wks post-treatment, the saline-treated EE and JHW007-treated mice induced improvement of rotarod performance relative to the saline-treated control mice. (B) Immunoprecipitation (IP) for phosphorylation of DAT and for interaction between DAT. The levels of the DAT phosphorylation bound with DAT significantly increased in SH-SY5Y cells after DAT inhibitor treatment (n=3 each).

11. Synaptophysin did not increase in striatum after EE

Many previous studies reported that EE conditions enhanced dendritic branching and new synapse formation in the brain.[2,3] To confirm for synaptic plasticity after long-term exposed EE, the expressions of presynaptic marker synaptophysin in striatum and frontal cortex were confirmed by Western blotting (Figure 12). This result showed that there was no difference between the groups as seen by confirmed the expression of synaptophysin in striatum. However, the expressions of synaptophysin in frontal cortex tend to increase after long-term exposure to EE.

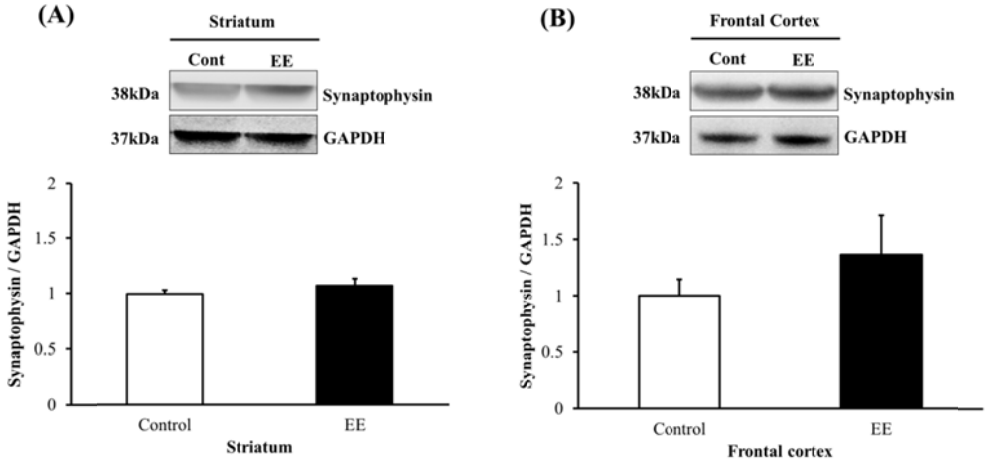

Figure 12. Expressions of synaptophysin in the striatum and frontal cortex. (A) Western blotting analysis confirmed the levels of the synaptophysin in EE, showing the level of the synaptophysin in EE had no difference with control group in striatum (B) The levels of the synaptophysin in EE, showing the level of the synaptophysin tend to increase in frontal cortex.

12. Distribution of DAT on the coronal slice from mice brain

To examine the location of DAT existence in multiple regions, mice brain sections were stained with anti-DAT antibody. Coronal slices were incubated to label with anti-DAT-Nt antibody, followed by secondary antibody conjugated with Alexa Fluor 488, or Alexa Fluor 594 respectively. The sections were imaged at low magnification using a confocal scanning microscope to assess labeling in the entire slice (Figure 13). The immunohistochemstry images showed that DAT mainly existed in higher concentration in striatal region such as caudate putamen. Dopaminergic neuronal cell bodies existed in SNc and VTA.

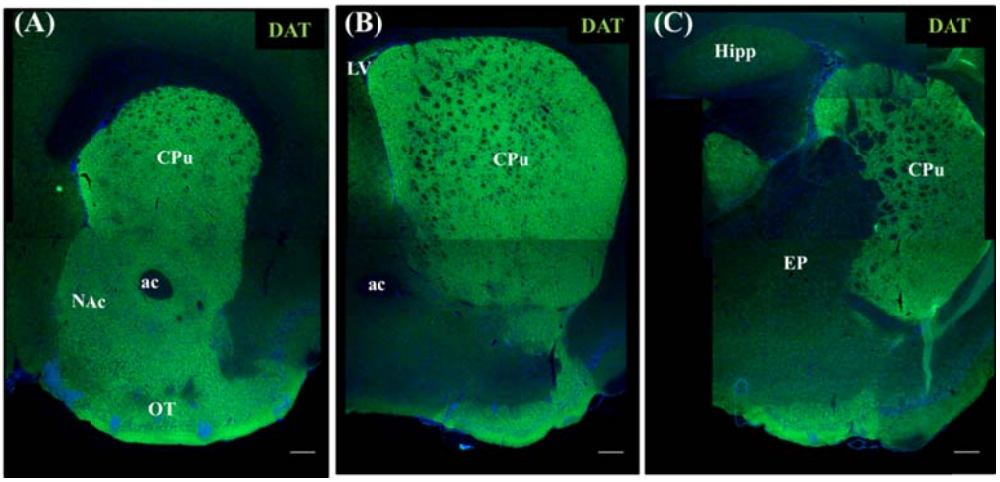

Scale bar = 200 ㎛

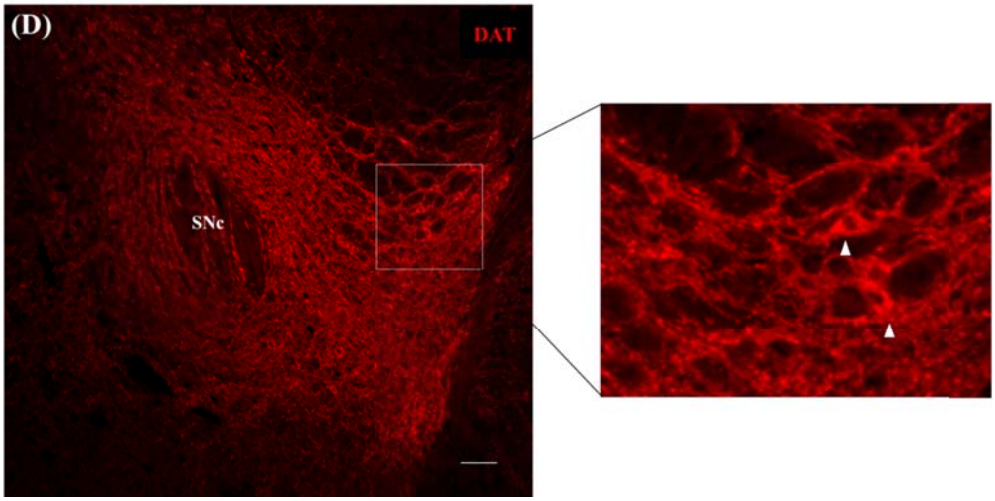

Scale bar = 100 ㎛

Figure 13. Distribution of DAT from mouse brain. Multiple regions were imaged using a scanning confocal system. Insets represent high-contrast images of the regions of (A) caudate putamen (Cpu), nucleus accumbens (NAc), olfactory tubercle (OT), (B) and (C) Cpu (D) substance nigra (SNc) indicated.

* ac : anterior commissure; EP : entopeduncular nucleus; Hipp : hippocampus; LV : lateral ventricle.

13. Location of DAT presynaptic and postsynaptic in striatum

To study the location of DAT existence in striatum, brain sections of the control and EE mice were stained with synaptophysin and postsynaptic density protein 95 (PSD95) (Figure 14A-D). Therefore, these confocal images showed that DAT existed in the presynaptic region by antibodies, such as co-localized synaptophysin and dopamine transporter. The striatum was stained with the dopamine transporter antibody as controls in dopamine transporter knock-out mice (B6N(Cg)-Slc6a3$^{tm1b(KOMP)Wtsi}$/J). (Figure 14E-F)

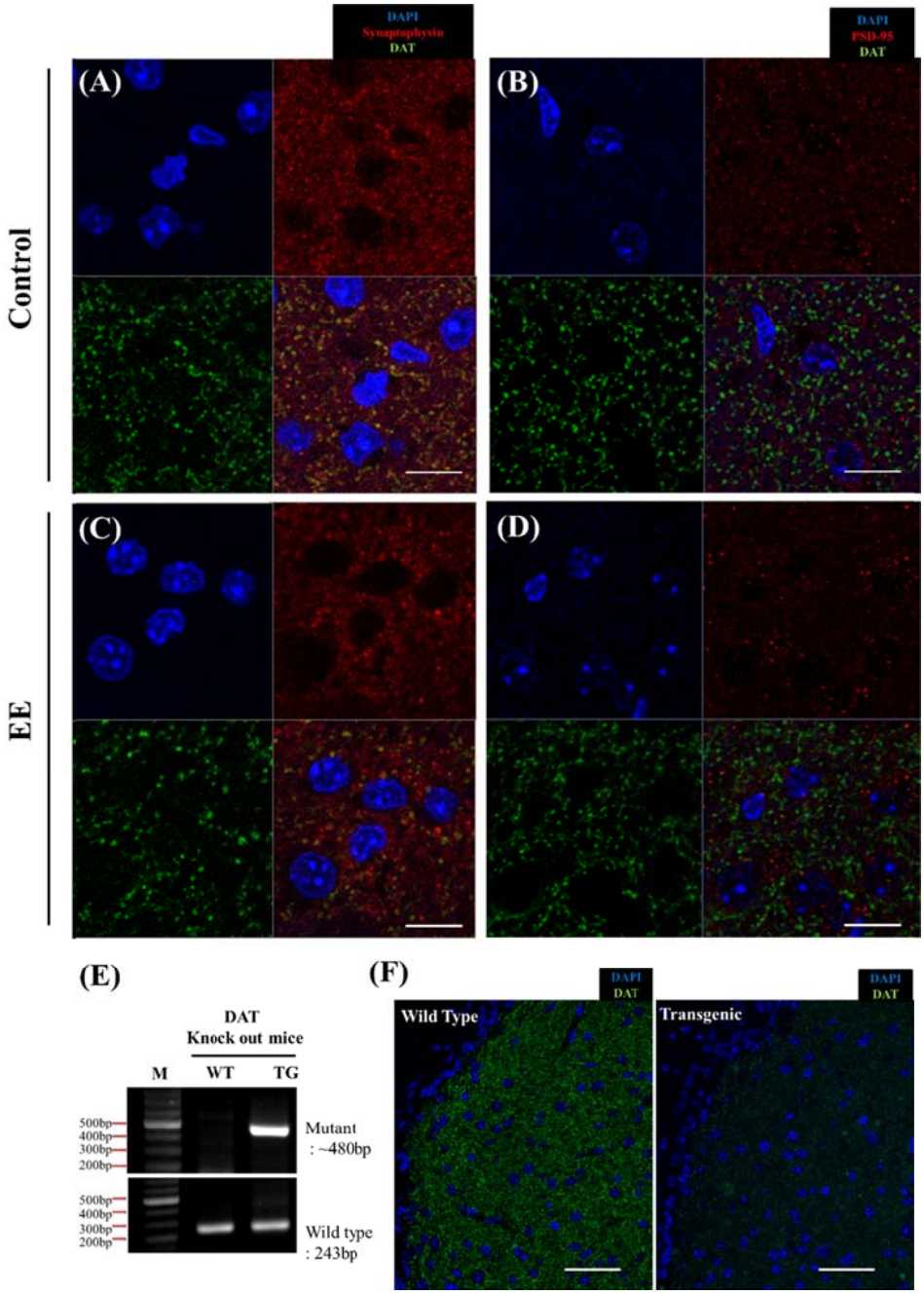

Figure 14. Dopamine transporters and synaptophysin co-localize in the striatum of control and EE mice. Confocal images showed co-localized DAT (Green) and synaptophysin (red) in the Control mice (A) and EE mice (B). However, DAT (Green) and PSD-95(red) were not co-localized in the Control mice (C) and EE mice (D) Scale bar = 10μm. (E) Genotyping result of DAT knock-out mice. The Mutant band was approximately ~ 480 bp, and Wild type was 243 bp. Confocal images showed dopamine transporter (Green) in the striatum of wild type and transgenic mice (F) Scale bar = 50 μm

IV. DISCUSSION

Both enhanced physical activity and social interaction provide benefits to the brain; physical activity on its own improves cognitive performance due to a range of neural changes including synaptic plasticity and neurotransmitter subunit expression.[53] However, the underlying mechanism remains to be elucidated in detail.

Therefore, to investigate the novel mechanisms that were regulated by exposure to EE, this study interpreted both microarray data and GSEA results. Among the biological functions of interest in the microarray data, PDYN, Ppp1r1b, and Slc6a3 in the neuronal activity category were statistically regulated by EE exposure. These genes contributed to the effects on opioid signaling and Na^+/Cl^--dependent transporters in the GSEA results. The PDYN and Ppp1r1b genes involved in opioid signaling were globally upregulated in the EE group.[49-51]

Among the genes involved in Na^+/Cl^--dependent neurotransmitter transporters, the Slc6a3 gene is a DAT that is a member of the Na^+/Cl^--dependent neurotransmitter transporter family. Slc6a3 is an integral membrane protein that removes dopamine from the synaptic cleft and deposits it into surrounding cells, thus terminating the signal of the neurotransmitter. The Slc6a3 gene involved in Na^+/Cl^--dependent neurotransmitter transporters was globally downregulated in the EE group; downregulating the expression of Slc6a3 leads to the increased synaptic occupancy of dopamine. It is interesting to note that the GSEA results demonstrated that dopamine neurotransmitter release was significantly downregulated after long-term exposure to EE. Among the genes related to dopamine release, tyrosine hydroxylase (TH) and dopa decarboxylase (DDC) genes were downregulated by EE.

In the intersection of microarray and GSEA results, this study suggest that dopamine biosynthesis was reduced and the bioactivity of neurotransmitters in the synaptic cleft was increased.

Rampon et al[7] previously described the effects of EE on the gene expression in the brain using oligonucleotide microarrays. They found that the expressions of genes associated with neuronal structure, synaptic plasticity, and transmission were significantly changed by EE exposure. Among the neurotransmitters used in previous studies, the role of dopamine as an important neurotransmitter has come to light.[54-57] Dopamine is responsible for many functions including motor activity and movement. Previous studies reported that levodopa could enhance motor recovery after stroke patients and experimental stroke.[58,59] The dopamine levels in the neural synapse are controlled by DAT. DAT is a 12-transmembrane domain protein and a member of the SLC6 gene family of Na^+/Cl^--dependent neurotransmitter transporters that also includes serotonin, GABA, norepinephrine and glycine transporters.[10] DAT is a pump for dopamine, which takes the neurotransmitter out of the synapse back into the presynaptic neural cytosol, and dopamine reuptake via DAT controls the concentration of dopamine between presynaptic and postsynaptic neurons.[60,61] Proper dopaminergic function is dependent on the reuptake activity by DAT, which is the primary mechanism responsible for the control of the DA levels in the neural synapse.[31,32,62] In this way, DAT plays a primary role in terminating dopaminergic signaling and maintaining a releasable pool of dopamine.[57]

In this study, quantitative real-time PCR was performed to determine DAT expression levels in the mouse brain under EE. DAT significantly decreased after

long-term exposure to EE, and DAT RNA levels show similar down-regulated expression patterns with microarray. In this study, the EE-mediated mechanism of synaptic plasticity was further elucidated by internalization of striatal DAT. BG circuits in dopamine are thought to promote motor skill acquisition through reinforcement learning.[63,64] Moreover, dopamine is also involved beyond motor learning.[26,28-30]

The EE-induced functional improvement was related to DAT down-regulation in striatum which was confirmed by [^{18}F]FPCIT PET image assays and administration of a DAT inhibitor. [^{18}F]FPCIT that is a specific radiotracer for DAT was predominantly located in the striatum in the DAT-PET image assay. Other brain regions had very low radioactivity concentration.[65,66] Moreover, the extra-striatal uptakes in small mouse brain were easily affected by the neighboring structure and partial volume effect, causing overestimation. Therefore, there were very small differences of radioactivity between extra-striatal brain regions and cerebellum. The present study focused on the changes of available DAT in the plasma membrane rather than cerebral perfusion. In [^{18}F]FPCIT PET image assay, cerebral perfusion effect could be negligible, because reference tissue has little DAT and a time activity curve from reference tissue replaced the arterial blood. This methodology is previously validated and currently used in the clinical PET study for Parkinson's disease.[67]

This study confirmed the internalization of striatal DAT using a surface biotinylation assay, and focused on DAT regulation mechanisms such as internalization and phosphorylation.[33,56] This study also validated the DAT

inhibition occurred via phosphorylation mechanism with *in vitro* experiment. However, present study did not show that decreased DAT is associated with the increment of Drd1 and Drd2 in EE. Previous studies demonstrated that there was no evidence that EE influenced D2 receptor density, or the ratio of D2 receptor density to other receptor types,[68] and destruction of DAT in Parkinsonian animal model did not showed statistically significant increment of D2 receptors.[69]

DAT phosphorylation by multiple signaling systems causes DAT internalization.[70,71] It has been reported that changes in DAT activity and cell surface expression occur in response to diverse mechanisms including several kinases and phosphatases.[71-76] In addition, recent studies have shown that DAT and other neurotransmitter transporters are phosphoproteins which are regulated by protein kinases as a mechanism for maintaining synaptic neurotransmitter levels and neural signaling.[70-73,77]

DAT is exclusively expressed in dopaminergic neurons.[10,23] The cell bodies of dopamine neurons are located in the ventral mesencephalic region of the brain consisting of the SNc and VTA. From there, dopamine neurons send bundles of axons rostrally to the primarily innervate regions involved in controlling locomotion, such as dorsal striatum and nucleus accumbens, as well as to the frontal cortex.[10,14,24] Specially, DAT is present in higher concentrations in striatal axons, presynaptic terminals in particular, thus suggesting the existence of a specific targeting mechanism, and there is a relatively small endolysosomal pool of DAT, which indicates the importance of both nonvesicular lateral membrane movement of the transporter, as well as plasma membrane retention mechanisms.[14] Previous

studies demonstrated that cell surface retention of DAT is controlled by juxtamembrane amino acid residues of the DAT-Nt.[78]

Animal models have played a major part in the improvement of our understanding of the underlying mechanisms of exercise and its effects on restoration of motor behavior in the dopamine-depleted brain. Exercise can restore important circuits in motor behavior by modulation of dopamine and glutamate neurotransmission and also affects general brain health.[7]

DAT can participate in the dopamine clearance only when it is present on the plasma membrane. DAT plasma membrane expression is regulated by the process of endocytosis.[10,51,74] DAT is thought to undergo constitutive and regulated endocytosis. [10,20] Many Studies indicate that PKC activation leads to endocytosis of DAT through clathrin coated pits[10,18,19] and accumulation of the transporter in early, recycling and late endosomes.[10,19,21,22] PKC reduces the rate of DAT plasma membrane recycling, further enhancing the level of transporter internalization.[33,72] PKC-dependent phosphorylation of DAT has been demonstrated at sites that appear to be the most distal N-terminal serine.[52] Present study evaluated DAT bound with PKCβ because it has been reported that PKCβ, but not PKCα or PKCγ, was co-immunoprecipitated with the DAT from striatal membranes.[47]

In this study, IP and *in situ* proximity assay demonstrated that EE increased phosphorylation of DAT via a PKC-mediated pathway as a DAT internalization mechanism, suggesting that EE caused DAT internalization by phosphorylation. As a result of DAT internalization and dopamine reuptake inhibition in the presynaptic region, increased levels of dopamine in the neural synapse might lead to functional

improvement. After this internalization, DAT undergoes several biological processes including degradation and recycling. The internalization process may play a key role in the intercellular regulation of DAT. Therefore, this study focused on the role of EE in the early steps of DAT trafficking, and showed that EE substantially increased DAT phosphorylation.

Experience-dependent plasticity is thought to involve selective change in pre-existing brain circuits, involving synaptic plasticity.[79] Previous studies showed that EE resulted in synaptic plasticity in the visual cortex[80] and hippocampus.[81,82] Recent study reported that EE resulted in increased synaptic proteins such as synaptophysin and PSD95 through major brain regions, including the forebrain, hippocampus, thalamus, and hypothalamus.[79] These results demonstrate that EE results in an increase in levels of both pre- and post-synaptic proteins in multiple regions of the brain, and it is possible that such changes represent the underlying synaptic plasticity occurring in EE.[79]

In this study tested the effects of EE and synaptic protein level via western blotting for synaptophysin. Western blotting result demonstrated that EE resulted in increased synaptophisin level through frontal cortex region. However, no changes in synaptophysin were detected in the striatum. This result showed that EE have distinct effects on synaptic alterations in brain region associated to motor function such as frontal cortex and striatum. This study suggests that DAT was influenced more by EE than dopamine receptor or synaptic protein.

Taken together, this study suggests that EE enables phosphorylation of DAT via a PKC-mediated pathway in the striatum. This is the first report to suggest the EE-mediated mechanism of synaptic plasticity by internalization of striatal DAT.

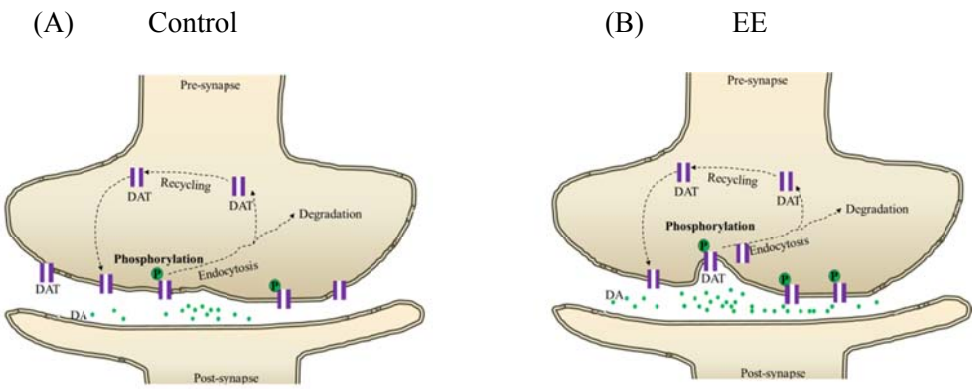

Figure 15. EE mediated internalization of DAT by phosphorylation in the presynaptic zone. As a result of DAT internalization and dopamine reuptake inhibition in the presynaptic region, dopamine levels in the neural synapse increased in the EE group (B) relative to the control group (A), which might cause functional improvement. After this internalization, DAT may undergo several biological processes including degradation and recycling. This internalization process plays a key role in the intercellular regulation of DAT. Therefore, we focused on the role of EE in the early steps of DAT trafficking, and showed that EE substantially increased DAT phosphorylation. Taken together, EE enables phosphorylation of DAT via a PKC-mediated pathway in the striatum, suggesting the EE-mediated mechanism of synaptic plasticity by internalization of striatal DAT.

V. CONCLUSION

This study aimed to investigate dopamine-related synaptic plasticity underlying functional improvements after EE. In conclusion, this study focused on the role of EE in the early steps of DAT trafficking, and showed that EE substantially increased DAT phosphorylation. Taken together, this study suggests that EE enables phosphorylation of DAT via a PKC-mediated pathway in the striatum.

REFERNCE

1. Rosenzweig MR, Bennett EL, Hebert M, Morimoto H. Social grouping cannot account for cerebral effects of enriched environments. Brain Res 1978;153:563-76.
2. van Praag H, Kempermann G, Gage FH. Neural consequences of environmental enrichment. Nat Rev Neurosci 2000;1:191-8.
3. Benaroya-Milshtein N, Hollander N, Apter A, Kukulansky T, Raz N, Wilf A, et al. Environmental enrichment in mice decreases anxiety, attenuates stress responses and enhances natural killer cell activity. Eur J Neurosci 2004;20:1341-7.
4. Will B, Galani R, Kelche C, Rosenzweig MR. Recovery from brain injury in animals: relative efficacy of environmental enrichment, physical exercise or formal training (1990-2002). Prog Neurobiol 2004;72:167-82.
5. Cummins RA, Walsh RN, Budtz-Olsen OE, Konstantinos T, Horsfall CR. Environmentally-induced changes in the brains of elderly rats. Nature 1973;243:516-8.
6. Abrous DN, Koehl M, Le Moal M. Adult neurogenesis: from precursors to network and physiology. Physiol Rev 2005;85:523-69.
7. Rampon C, Jiang CH, Dong H, Tang YP, Lockhart DJ, Schultz PG, et al. Effects of environmental enrichment on gene expression in the brain. Proc Natl Acad Sci U S A 2000;97:12880-4.
8. Leal-Galicia P, Castaneda-Bueno M, Quiroz-Baez R, Arias C. Long-term exposure to environmental enrichment since youth prevents recognition memory decline and increases synaptic plasticity markers in aging. Neurobiol Learn Mem 2008;90:511-8.
9. Zhu SW, Yee BK, Nyffeler M, Winblad B, Feldon J, Mohammed AH. Influence of differential housing on emotional behaviour and neurotrophin levels in mice. Behav Brain Res 2006;169:10-20.
10. Mlynarik M, Johansson BB, Jezova D. Enriched environment influences adrenocortical response to immune challenge and glutamate receptor gene expression in rat hippocampus. Ann N Y Acad Sci 2004;1018:273-80.
11. Branchi I, D'Andrea I, Fiore M, Di Fausto V, Aloe L, Alleva E. Early social enrichment shapes social behavior and nerve growth factor and brain-derived neurotrophic factor levels in the adult mouse brain. Biol Psychiatry 2006;60:690-6.
12. Rossi C, Angelucci A, Costantin L, Braschi C, Mazzantini M, Babbini F, et al. Brain-derived neurotrophic factor (BDNF) is required for the enhancement of hippocampal neurogenesis following environmental enrichment. Eur J Neurosci 2006;24:1850-6.
13. Staiger JF, Masanneck C, Bisler S, Schleicher A, Zuschratter W, Zilles K. Excitatory and inhibitory neurons express c-Fos in barrel-related columns after exploration of a novel environment. Neuroscience 2002;109:687-99.

14. Williams BM, Luo Y, Ward C, Redd K, Gibson R, Kuczaj SA, et al. Environmental enrichment: effects on spatial memory and hippocampal CREB immunoreactivity. Physiol Behav 2001;73:649-58.
15. Nithianantharajah J, Hannan AJ. Enriched environments, experience-dependent plasticity and disorders of the nervous system. Nat Rev Neurosci 2006;7:697-709.
16. Rosenzweig MR, Bennett EL. Psychobiology of plasticity: effects of training and experience on brain and behavior. Behav Brain Res 1996;78:57-65.
17. Seo JH, Yu JH, Suh H, Kim MS, Cho SR. Fibroblast growth factor-2 induced by enriched environment enhances angiogenesis and motor function in chronic hypoxic-ischemic brain injury. PLoS One 2013;8:e74405.
18. Thanos PK, Hamilton J, O'Rourke JR, Napoli A, Febo M, Volkow ND, et al. Dopamine D2 gene expression interacts with environmental enrichment to impact lifespan and behavior. Oncotarget 2016; doi:10.18632/oncotarget.8088.
19. Mora F, Segovia G, del Arco A. Aging, plasticity and environmental enrichment: structural changes and neurotransmitter dynamics in several areas of the brain. Brain Res Rev 2007;55:78-88.
20. Aumann TD. Environment- and activity-dependent dopamine neurotransmitter plasticity in the adult substantia nigra. J Chem Neuroanat 2016;73:21-32.
21. Roth RH, Tam SY, Ida Y, Yang JX, Deutch AY. Stress and the mesocorticolimbic dopamine systems. Ann N Y Acad Sci 1988;537:138-47.
22. Feenstra MG, Botterblom MH. Rapid sampling of extracellular dopamine in the rat prefrontal cortex during food consumption, handling and exposure to novelty. Brain Res 1996;742:17-24.
23. Tidey JW, Miczek KA. Social defeat stress selectively alters mesocorticolimbic dopamine release: an in vivo microdialysis study. Brain Res 1996;721:140-9.
24. Segovia G, Del Arco A, de Blas M, Garrido P, Mora F. Effects of an enriched environment on the release of dopamine in the prefrontal cortex produced by stress and on working memory during aging in the awake rat. Behav Brain Res 2008;187:304-11.
25. Calabresi P, Centonze D, Bernardi G. Electrophysiology of dopamine in normal and denervated striatal neurons. Trends Neurosci 2000;23:S57-63.
26. Leblois A, Wendel BJ, Perkel DJ. Striatal dopamine modulates basal ganglia output and regulates social context-dependent behavioral variability through D1 receptors. J Neurosci 2010;30:5730-43.
27. Smith Y, Villalba R. Striatal and extrastriatal dopamine in the basal ganglia: an overview of its anatomical organization in normal and Parkinsonian brains. Mov Disord 2008;23 Suppl 3:S534-47.
28. Wang Z, Yu G, Cascio C, Liu Y, Gingrich B, Insel TR. Dopamine D2 receptor-mediated regulation of partner preferences in female prairie voles

(Microtus ochrogaster): a mechanism for pair bonding? Behav Neurosci 1999;113:602-11.
29. Anstrom KK, Miczek KA, Budygin EA. Increased phasic dopamine signaling in the mesolimbic pathway during social defeat in rats. Neuroscience 2009;161:3-12.
30. Aragona BJ, Liu Y, Curtis JT, Stephan FK, Wang Z. A critical role for nucleus accumbens dopamine in partner-preference formation in male prairie voles. J Neurosci 2003;23:3483-90.
31. Zhu J, Apparsundaram S, Bardo MT, Dwoskin LP. Environmental enrichment decreases cell surface expression of the dopamine transporter in rat medial prefrontal cortex. J Neurochem 2005;93:1434-43.
32. Wooters TE, Bardo MT, Dwoskin LP, Midde NM, Gomez AM, Mactutus CF, et al. Effect of environmental enrichment on methylphenidate-induced locomotion and dopamine transporter dynamics. Behav Brain Res 2011;219:98-107.
33. Foster JD, Yang JW, Moritz AE, Challasivakanaka S, Smith MA, Holy M, et al. Dopamine transporter phosphorylation site threonine 53 regulates substrate reuptake and amphetamine-stimulated efflux. J Biol Chem 2012;287:29702-12.
34. Lee MY, Yu JH, Kim JY, Seo JH, Park ES, Kim CH, et al. Alteration of synaptic activity-regulating genes underlying functional improvement by long-term exposure to an enriched environment in the adult brain. Neurorehabil Neural Repair 2013;27:561-74.
35. Metz GA, Whishaw IQ. The ladder rung walking task: a scoring system and its practical application. J Vis Exp 2009; doi:10.3791/1204.
36. Na HN, Kim H, Nam JH. Novel genes and cellular pathways related to infection with adenovirus-36 as an obesity agent in human mesenchymal stem cells. Int J Obes (Lond) 2012;36:195-200.
37. Kim H, Cho HJ, Kim SW, Liu B, Choi YJ, Lee J, et al. CD31+ cells represent highly angiogenic and vasculogenic cells in bone marrow: novel role of nonendothelial CD31+ cells in neovascularization and their therapeutic effects on ischemic vascular disease. Circ Res 2010;107:602-14.
38. Subramanian A, Tamayo P, Mootha VK, Mukherjee S, Ebert BL, Gillette MA, et al. Gene set enrichment analysis: a knowledge-based approach for interpreting genome-wide expression profiles. Proc Natl Acad Sci U S A 2005;102:15545-50.
39. Lee SJ, Oh SJ, Chi DY, Kang SH, Kil HS, Kim JS, et al. One-step high-radiochemical-yield synthesis of [18F]FP-CIT using a protic solvent system. Nucl Med Biol 2007;34:345-51.
40. Constantinescu CC, Mukherjee J. Performance evaluation of an Inveon PET preclinical scanner. Phys Med Biol 2009;54:2885-99.
41. George P WC, editor. The rat brain in stereotaxic coordinates. San Diego, CA.; 2007.

42. Boja JW, Mitchell WM, Patel A, Kopajtic TA, Carroll FI, Lewin AH, et al. High-affinity binding of [125I]RTI-55 to dopamine and serotonin transporters in rat brain. Synapse 1992;12:27-36.
43. Cline EJ, Scheffel U, Boja JW, Mitchell WM, Carroll FI, Abraham P, et al. In vivo binding of [125I]RTI-55 to dopamine transporters: pharmacology and regional distribution with autoradiography. Synapse 1992;12:37-46.
44. Agoston GE, Wu JH, Izenwasser S, George C, Katz J, Kline RH, et al. Novel N-substituted 3 alpha-[bis(4'-fluorophenyl)methoxy]tropane analogues: selective ligands for the dopamine transporter. J Med Chem 1997;40:4329-39.
45. Velazquez-Sanchez C, Ferragud A, Murga J, Carda M, Canales JJ. The high affinity dopamine uptake inhibitor, JHW 007, blocks cocaine-induced reward, locomotor stimulation and sensitization. Eur Neuropsychopharmacol 2010;20:501-8.
46. Soderberg O, Gullberg M, Jarvius M, Ridderstrale K, Leuchowius KJ, Jarvius J, et al. Direct observation of individual endogenous protein complexes in situ by proximity ligation. Nat Methods 2006;3:995-1000.
47. Johnson LA, Guptaroy B, Lund D, Shamban S, Gnegy ME. Regulation of amphetamine-stimulated dopamine efflux by protein kinase C beta. J Biol Chem 2005;280:10914-9.
48. Furman CA, Chen R, Guptaroy B, Zhang M, Holz RW, Gnegy M. Dopamine and amphetamine rapidly increase dopamine transporter trafficking to the surface: live-cell imaging using total internal reflection fluorescence microscopy. J Neurosci 2009;29:3328-36.
49. Werme M, Thoren P, Olson L, Brene S. Running and cocaine both upregulate dynorphin mRNA in medial caudate putamen. Eur J Neurosci 2000;12:2967-74.
50. Stagg NJ, Mata HP, Ibrahim MM, Henriksen EJ, Porreca F, Vanderah TW, et al. Regular exercise reverses sensory hypersensitivity in a rat neuropathic pain model: role of endogenous opioids. Anesthesiology 2011;114:940-8.
51. Boecker H, Sprenger T, Spilker ME, Henriksen G, Koppenhoefer M, Wagner KJ, et al. The runner's high: opioidergic mechanisms in the human brain. Cereb Cortex 2008;18:2523-31.
52. Foster JD, Pananusorn B, Vaughan RA. Dopamine transporters are phosphorylated on N-terminal serines in rat striatum. J Biol Chem 2002;277:25178-86.
53. Farmer J, Zhao X, van Praag H, Wodtke K, Gage FH, Christie BR. Effects of voluntary exercise on synaptic plasticity and gene expression in the dentate gyrus of adult male Sprague-Dawley rats in vivo. Neuroscience 2004;124:71-9.
54. Carlsson A, Lindqvist M, Magnusson T. 3,4-Dihydroxyphenylalanine and 5-hydroxytryptophan as reserpine antagonists. Nature 1957;180:1200.
55. Carlsson A, Lindqvist M, Magnusson T, Waldeck B. On the presence of 3-hydroxytyramine in brain. Science 1958;127:471.

56. Montagu KA. Catechol compounds in rat tissues and in brains of different animals. Nature 1957;180:244-5.
57. Eriksen J, Jorgensen TN, Gether U. Regulation of dopamine transporter function by protein-protein interactions: new discoveries and methodological challenges. J Neurochem 2010;113:27-41.
58. Scheidtmann K, Fries W, Muller F, Koenig E. Effect of levodopa in combination with physiotherapy on functional motor recovery after stroke: a prospective, randomised, double-blind study. Lancet 2001;358:787-90.
59. Ruscher K, Kuric E, Wieloch T. Levodopa treatment improves functional recovery after experimental stroke. Stroke 2012;43:507-13.
60. Manepalli S, Surratt CK, Madura JD, Nolan TL. Monoamine transporter structure, function, dynamics, and drug discovery: a computational perspective. Aaps j 2012;14:820-31.
61. Pramod AB, Foster J, Carvelli L, Henry LK. SLC6 transporters: structure, function, regulation, disease association and therapeutics. Mol Aspects Med 2013;34:197-219.
62. Shan J, Javitch JA, Shi L, Weinstein H. The substrate-driven transition to an inward-facing conformation in the functional mechanism of the dopamine transporter. PLoS One 2011;6:e16350.
63. Hikosaka O, Nakamura K, Sakai K, Nakahara H. Central mechanisms of motor skill learning. Curr Opin Neurobiol 2002;12:217-22.
64. Graybiel AM. The basal ganglia: learning new tricks and loving it. Curr Opin Neurobiol 2005;15:638-44.
65. Malison RT, Vessotskie JM, Kung MP, McElgin W, Romaniello G, Kim HJ, et al. Striatal dopamine transporter imaging in nonhuman primates with iodine-123-IPT SPECT. J Nucl Med 1995;36:2290-7.
66. Lundkvist C, Halldin C, Ginovart N, Swahn CG, Farde L. [18F] beta-CIT-FP is superior to [11C] beta-CIT-FP for quantitation of the dopamine transporter. Nucl Med Biol 1997;24:621-7.
67. Yaqub M, Boellaard R, van Berckel BN, Ponsen MM, Lubberink M, Windhorst AD, et al. Quantification of dopamine transporter binding using [18F]FP-beta-CIT and positron emission tomography. J Cereb Blood Flow Metab 2007;27:1397-406.
68. Anderson BJ, Gatley SJ, Rapp DN, Coburn-Litvak PS, Volkow ND. The ratio of striatal D1 to muscarinic receptors changes in aging rats housed in an enriched environment. Brain Res 2000;872:262-5.
69. Choi JY, Kim CH, Jeon TJ, Cho WG, Lee JS, Lee SJ, et al. Evaluation of dopamine transporters and D2 receptors in hemiparkinsonian rat brains in vivo using consecutive PET scans of [18F]FPCIT and [18F]fallypride. Appl Radiat Isot 2012;70:2689-94.
70. Ramamoorthy S, Shippenberg TS, Jayanthi LD. Regulation of monoamine transporters: Role of transporter phosphorylation. Pharmacol Ther 2011;129:220-38.

71. Ramamoorthy S, Blakely RD. Phosphorylation and sequestration of serotonin transporters differentially modulated by psychostimulants. Science 1999;285:763-6.
72. Vaughan RA, Huff RA, Uhl GR, Kuhar MJ. Protein kinase C-mediated phosphorylation and functional regulation of dopamine transporters in striatal synaptosomes. J Biol Chem 1997;272:15541-6.
73. Vaughan RA, Foster JD. Mechanisms of dopamine transporter regulation in normal and disease states. Trends Pharmacol Sci 2013;34:489-96.
74. Pristupa ZB, McConkey F, Liu F, Man HY, Lee FJ, Wang YT, et al. Protein kinase-mediated bidirectional trafficking and functional regulation of the human dopamine transporter. Synapse 1998;30:79-87.
75. Chen R, Furman CA, Gnegy ME. Dopamine transporter trafficking: rapid response on demand. Future Neurol 2010;5:123.
76. Moron JA, Zakharova I, Ferrer JV, Merrill GA, Hope B, Lafer EM, et al. Mitogen-activated protein kinase regulates dopamine transporter surface expression and dopamine transport capacity. J Neurosci 2003;23:8480-8.
77. Torres GE. The dopamine transporter proteome. J Neurochem 2006;97 Suppl 1:3-10.
78. Montague PR, Dayan P, Sejnowski TJ. A framework for mesencephalic dopamine systems based on predictive Hebbian learning. J Neurosci 1996;16:1936-47.
79. Nithianantharajah J, Levis H, Murphy M. Environmental enrichment results in cortical and subcortical changes in levels of synaptophysin and PSD-95 proteins. Neurobiol Learn Mem 2004;81:200-10.
80. Turner AM, Greenough WT. Differential rearing effects on rat visual cortex synapses. I. Synaptic and neuronal density and synapses per neuron. Brain Res 1985;329:195-203.
81. Moser MB, Trommald M, Andersen P. An increase in dendritic spine density on hippocampal CA1 pyramidal cells following spatial learning in adult rats suggests the formation of new synapses. Proc Natl Acad Sci U S A 1994;91:12673-5.
82. Rampon C, Tang YP, Goodhouse J, Shimizu E, Kyin M, Tsien JZ. Enrichment induces structural changes and recovery from nonspatial memory deficits in CA1 NMDAR1-knockout mice. Nat Neurosci 2000;3:238-44.

ABSTRACT (IN KOREAN)

풍요 환경에 의한 도파민 수송자의 내재화에 따른 시냅스 가소성 및 기능 강화

<지도교수 조성래>

연세대학교 대학원 의과학과

유지혜

물리적, 인지적 그리고 사회적 자극들의 다양한 조합으로 이루어져 있는 풍요환경(EE)은 시냅스 가소성과 행동학적 기능을 강화시킨다. 그러나 이러한 강화에 대한 자세한 기전은 밝혀지지 않은 상태이다. 그래서 이 연구에서는 유전자 발현 패턴을 평가하여 장기적인 풍요 환경의 노출과 관련된 기전을 밝히고자 하였으며 더 나아가 풍요 환경 이후 기능 강화에 관련되어 도파민과 연관된 시냅스 가소성을 밝히고자 하였다. 이를 위해 6 주령의 CD-1 행동학적 기능 결과를 관찰 하기 위하여 무작위로 풍요 환경과 대조 환경으로 나누어 사육하였다. 풍요환경 쥐들은 대형 사육장 (86×76×31 cm^3) 에서 2 달간 사육하였고

반면 대조군은 표준 사육장 (27×22.5×14 cm^3)에서 사육하였다. 운동 기능을 평가하기 위해 로타로드(rotarod)와 사다리 걷기 검사(ladder walking test)를 사용하였고 유전자 발현 개요를 밝히기 위해 대뇌 반구에서 마이크로어레이와 gene set enrichment analysis(GSEA)을 이용하였다. 바이오티닐(biontinylation) 분석법을 이용하여 표면 도파민 수송자를, proximity ligation assay(PLA)와 면역침강법을 통해 도파민 수송자의 인산화를, [^{18}F]FPCIT 양전자방출단층촬영술을 이용하여 선조체 도파민 수송자를 평가하기 위해 대상들을 모집하였다. 풍요 환경 8 주 후, 풍요 환경군이 로타로드와 사다리 걷기검사와 같은 행동학적 기능에서 유의하게 강화되었다. 마이크로어레이 분석에서 풍요 환경에 의해 신경 활동에 관련된 유전자들이 유의하게 변화된 것이 드러났다. GSEA 분석에서 시냅스 간의 전달과 시냅스 후 신호 변환에 관련된 유전자들이 전반적으로 상향조절 되었지만 시냅스 후 신경전달물질 수송자에 의한 재흡수는 하향조절 되는 것이 보여졌다. 특히 마이크로어레이와 GSEA 에서 풍요 환경 노출에서 오피오이드 신호, 아세트콜린 분비 순환, 시냅스 후 신경전달물질 수용체가 증가하지만 뇌에서 도파민 수송자인 Slc6a3 을 포함하는 Na^+/Cl^- 의존적 신경전달물질 수송자는 감소하였다. 선조체는 뇌에서 가장 큰 도파민 입력을 받는 곳이며 도파민 시스템은 운동 수행 같은 움직임을 포함한다. 그래서 이

연구에서는 풍요 환경에 의해 유도된 기능 강화가 선조체에서 도파민 수송자의 하향조절과 관련되었는지 조사하였다.

[^{18}F]FPCIT 양전자방출단층촬영술에서 선조체 도파민 수송자에 붙는 수치는 풍요 환경에서 사육된 쥐들이 대조 환경에서 사육된 쥐들에 대비하여 대략 18% 가 유의성 있게 감소하였다. 도파민 수송자 억제제를 투여하여 도파민 수송자의 감소로 인한 치료 효과와 로타로드와 같은 운동 기능 강화의 관계를 밝히고자 하였으며 이는 도파민 수송자의 억제가 풍요 환경이 영향을 주는 개요를 뒷받침 하였다. 다음으로 풍요환경이 유도하는 도파민 수송자의 내재화를 표면 바이오티닐(biotinyl) 분석법을 사용하여 확인하였다. *In situ* proximity ligation assay 와 면역침강법을 이용하여 풍요환경이 선조체 도파민 수송자의 인산화와 도파민 수송자와 붙는 단백질 인산화 효소 C (protein kinase C) 의 양이 유의성 있게 증가된 것을 확인하였다. 결론적으로 풍요환경은 시냅스후 수용체의 활동의 상향조절에 의한 시냅스 가소성과 신경전달물질의 효율적인 사용의 향상과 도파민 수송자와 같은 신경전달물질 수송자에 의한 시냅스전 재흡수의 하향조절 같은 시냅스 활동 조절에 관련된 유전자들의 변화를 통해 운동기능을 강화시킨다. 또한 이 연구는 단백질 인산화 효소 C 조절의 경로를 통해 선조체 도파민 수송자의 인산화를 가능하게 하며 이는 도파민 수송자의 내재화의 원인이 된다는 것을 제안하였다.

핵심되는 말 : 풍요 환경, 기능 강화, 도파민 수송자, 내재화, 인산화, 시냅스 가소성